BUDAPEST UNIVERSITY OF TECHNOLOGY AND ECONOMICS
FACULTY OF CIVIL ENGINEERING
DEPARTMENT OF STRUCTURAL MECHANICS

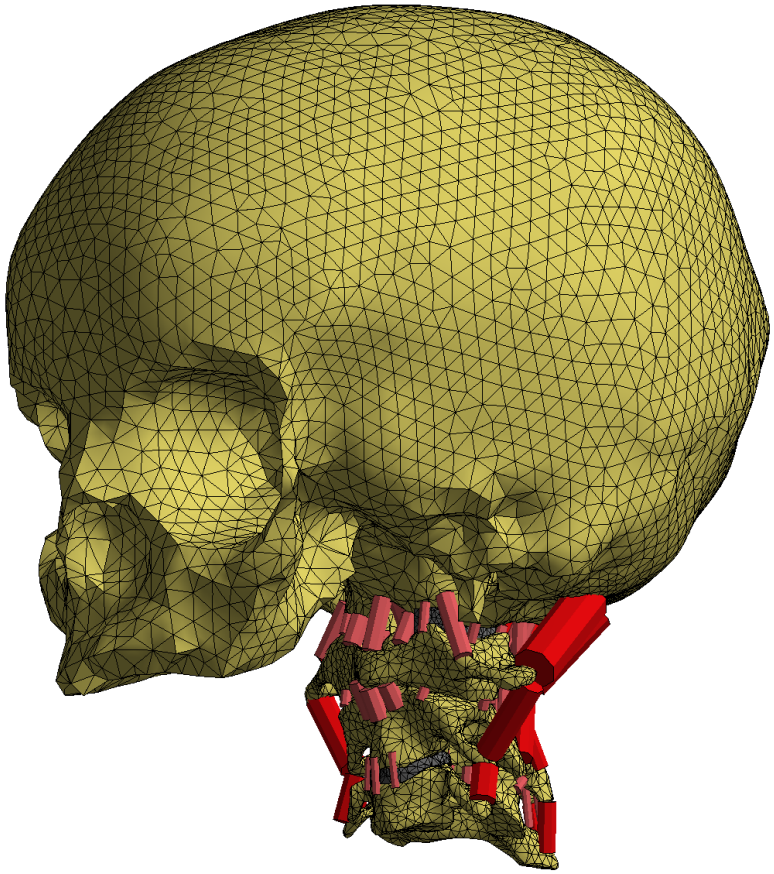

The Fracture of the Human Cervical Spine

Students' Scientific Conference

TDK report

Dávid Danka (H44CPZ)

Supervisors: Dr. Imre Bojtár, Máté Hazay

12. November 2019

SUMMARY

The interruption of the natural continuity of the cervical spine involves two types of lesions: fracture of the vertebrae and disruption of the connecting soft tissues. In some mild cases, the damage can be healed with well-established medical methods. However, since one of the main functions of the human cervical spine is to protect the spinal cord thus, when the protective tissues are damaged, the spinal cord may be easily injured, too, leading to serious consequences such as reduced neurological control, quadriplegia or fatality.

Frequently, such as during automobile collisions, the injury mechanism of the cervical spine is not precisely understood therefore we are not able to establish efficient and robust prevention, diagnostic or treatment methods. Hence, a detailed analysis is still necessary by modelling the spine and its components as accurately as possible with the help of present technical capabilities.

In the past, numerous experimental research were conducted with animal or cadaver surrogates. However, nowadays, one of the most commonly used numerical method to model the cervical spine is the finite element method, which provides access to the internal behavior of the cervical spine.

As it is evident, past investigations resulted in some preventive measures being already incorporated, for instance, the seat belt or the head rest, as far as the automotive industry is concerned. Nonetheless, we have other clues with regard to factors influencing the injury mechanism and severity.

There is still no complex mathematical model that fully takes the rather complicated inner structures of all tissues and their interaction into consideration, not to mention the exact modelling of the environment that causes lesions to the cervical spine.

The present study may be considered as a first step in a prolonged research task. As a beginning, my first goal is to develop a model with accurate anatomical structure and to prove its viability. The investigation of the complex, nonlinear relationship of bony segments, cartilaginous parts, ligaments and bones is dedicated to a part of a later step in this research task.

ÖSSZEFOGLALÓ

A nyaki gerinc folytonossága alapvetően két fajta sérülés hatására szakadhat meg: a csigolyák törése és a csigolyák közti kötő- illetve izomszövet széthasadása miatt. Enyhébb esetekben a sérülés megbízható orvosi módszerekkel gyógyítható. Mivel azonban az emberi nyaki gerinc fő funkciói közé tartozik a gerincvelő védelme, ezért amikor az azt védő szövetek sérülnek, a gerincvelő is könnyen megsérülhet, ami súlyos következményekkel járhat, nevezetesen: csökkent idegi kontrollal, bénulással vagy halállal.

Gyakran – például autóbaleseteknél – előfordul, hogy a nyaki gerinc sérülésének mechanizmusa behatóbban nem ismert, ezért nincs lehetőség hatékony módszereket kidolgozni, amelyekkel megelőzhetnénk, diagnosztizálhatnánk vagy kezelhetnénk a nyaki gerincet érő bármely sérülést. Ezért van szükség arra, hogy részletesen vizsgáljuk a gerinc mechanikai viselkedését, olyan pontosan modellezve az egyes alkotóelemeit, amennyire csak lehetséges a jelen technikai adottságok segítségével.

A korábbi évtizedekben számos kísérleti kutatást végeztek; manapság azonban az egyik leggyakrabban alkalmazott numerikus technika, amellyel modellezni igyekeznek az emberi nyaki gerincet, a végeselemes módszer, ami betekintést nyújt a gerinc belső, mechanikai működésébe.

Nyilvánvaló, hogy a korábbi tudományos vizsgálatok természetsen számos preventív intézkedés bevezetését tették lehetővé; az autóiparból hozva példát: ilyen, sérülést megelőző eszköz a biztonsági öv és a fejtámla. Ennek ellenére vannak még további jelek, amelyek különböző, a nyaki gerincet érő sérülések mechanizmusát és súlyosságát befolyásoló tényezőkre mutatnak.

Továbbra sem alkottak még meg egy olyan matematikai modellt, amely a nyaki gerinc összes – egyenként is meglehetősen komplikált – belső felépítő elemét, illetve ezek kölcsönhatását figyelembe venné; nem is beszélve a sérülést okozó környezet pontos modellezéséről.

Jelen dolgozat egy hosszabb kutatási munka első állomásának tekinthető. E munka első lépéseként az anatómiailag helyes modell megalkotása és működőképességének bizonyítása volt a célom. A csontok, porcos részek, inak és izmok bonyolult nemlineáris kapcsolatrendszerének vizsgálata egy következő feladat lesz számomra.

ACKNOWLEDGEMENTS

I owe many thanks to people who have made great contributions to the present study in various forms.

First, I feel deeply indebted to professor Bojtár. Not only his expertise in the scientific domain made my work possible but also his encouragement during every consultation. No matter how hard was the problem I faced related to the study, he always managed to get me back on track. I also appreciate the time he must have spent reading the text of this study and finding mistakes in it week after week.

Furthermore, I give huge thanks to Máté for his willingness to share his experiences related to the analysis software I used. He helped me moving over my stuck points of the software many-many times.

I am grateful for my parents and my sister, too. They accepted that I began to work on such a huge project and offered their cooperation and help immediately.

Last but not least, I must name one more individual who had great influence on my journey of writing this study: my bride. She encouraged me to keep working and do my best even though she didn't receive any short-term gain by doing that. I am not able to thank her support enough.

DENOTIONS

Vertebrae

- C# – cervical vertebra
- T# – thoracic vertebra
- L# – lumbar vertebra

Ligaments

- ALL – anterior longitudinal ligament
- PLL – posterior longitudinal ligament
- CL – capsular ligament
- LF – ligamentum flavum
- SL – supraspinous ligament
- LN – ligamentum nuchae
- ISL – interspinous ligaments
- ITL – intertransverse ligaments

Atlantoaxial ligaments

- AAAL – anterior atlantoaxial ligament
- PAAL – posterior atlantoaxial ligament
- TL – transverse ligament

Atlanto-occipital ligaments

- AAOM – anterior atlantooccipital membrane
- PAOM – posterior atlantooccipital membrane
- LL – lateral ligaments

Ligaments connecting the axis with the occiput

- TM – tectorial membrane
- AL – alar ligament
- AOL – apical odontoid ligament

Cervical muscles

- MIS – Muscle Interspinales
- MIT – Muscle Intertransversarii
- MR – Muscle Rotatores
- MRCPMi – Muscle Rectus Capitis Posterior Minor
- MOCS – Muscle Obliquus Capitis Superior

FDC – Force-displacement curve

TABLE OF CONTENTS

1. INTRODUCTION

In our age, after the automotive industry has largely accelerated transportation in general, a fair number of car accidents occur, some of which result in neck injury. Cervical spine injuries that cause quadriplegia, although not the most frequently occurring injury type, are devastating for the individual as well as for society and, additionally, rather costly. Beside the medical cost related to quadriplegia, there is also significant loss in productivity, both of which is estimated to be $97 billion in the USA (French et al., 2007), since mostly the young members of the society suffer severe injury. Thus, further investigation is still needed in order to prevent and treat these injuries efficiently.

Since the presented problem is a biomechanical one, a few basic descriptive anatomical concepts are explained shortly in **Anatomical background**. These concepts help describing the location of a part of an organ or a direction of a motion. Then the related anatomy of the cervical spine follows in greater detail in.

In the section of **Biomechanical analysis of the cervical spine**, an overview is given of the related scientific results concerning the human cervical spine. First, the constituent materials are introduced with their most important properties. Next, the basic aspects of the normal mechanical operation of the cervical spine is described. Based on this information, one may understand the injury mechanisms better in the following subsection. Then, cervical spine injuries are better explained in light of the injury mechanisms since these two are intimately related to each other. Finally, this part of the study ends with a broad overview of attempts of exploring the aforementioned phenomena with the help of laboratory tests and finite element models.

In the next section, **Development of the finite element model**, the general process of building the computational model is presented with regards to the geometry, material models, loads and boundary conditions. The scope of the present study is the computational analysis of the skull, the top three vertebrae and a few of the connecting soft tissues.

Next, in the part of **Numerical results**, the static as well as the dynamic analysis results are described and interpreted.

Finally, the summary of the whole work is found in **Conclusions**.

2. ANATOMICAL BACKGROUND

2.1. ANATOMICAL PLANES, AXES AND DIRECTIONS OF MOTIONS

Humans are capable of locomotion; this is the reason why a standard position of the body has to be agreed upon in order to simplify our description of the body (**Figure 1.**)

One of the concepts related to this standard position are the so called *anatomical planes*. The anatomical planes in general are not assigned to a specific point of the body, on which they lie, thus are not defined uniquely: only the orientation of the planes is fixed. This feature enables a flexible usage of the planes.

There's an exception to the above mentioned general concept: the position of the *median sagittal plane* is uniquely defined since it is identical to the only symmetry plane of the human body. Every plane that is parallel to the median sagittal plane is called, simply, *sagittal plane*. The *frontal plane* is parallel to the longitudinal axis of the body and perpendicular to the sagittal plane. The *transverse plane* is perpendicular to both currently introduced planes (Szentágothai and Réthelyi, 2006) (**Figure 1.**)

The next concept, which can be derived from the anatomical planes, are the *anatomical axes*. As far as the axes are concerned, the same flexible interpretation applies: their exact, unique position might be assigned to various points in the body, only their orientation is conventional. The three corresponding axes are formed by the appropriate planes (Lowe et al.,

2018): *sagittal axis* is the intersection of sagittal and transverse planes, *frontal axis* is the intersection of frontal and transverse planes, *longitudinal axis* is the intersection of sagittal and frontal planes.

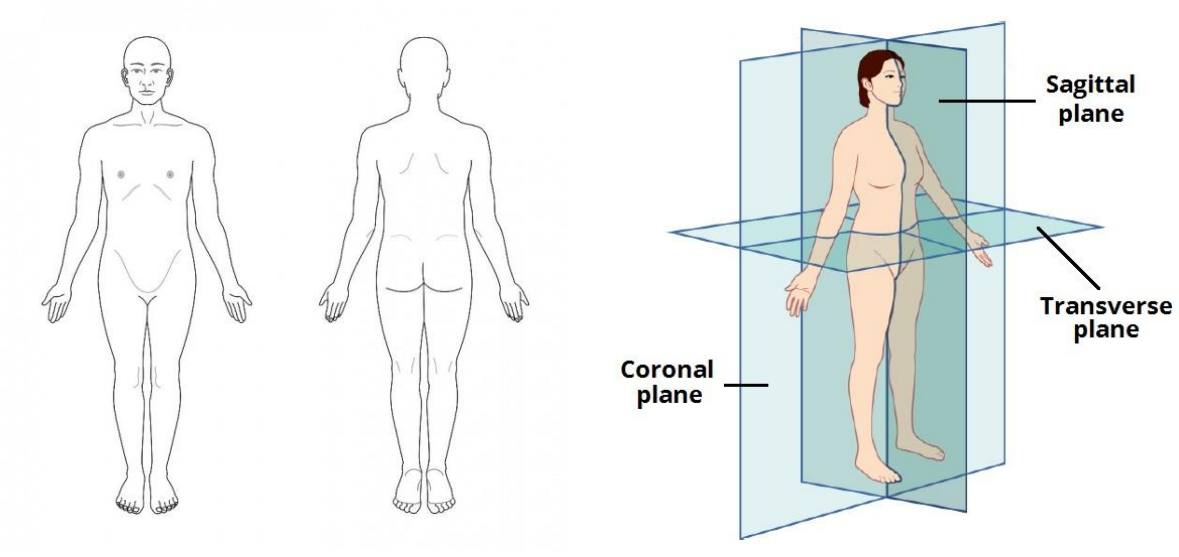

a) b)

Figure 1. a) Standard anatomical position (Lowe et al., 2018), b) Anatomical planes (Jones, 2012)

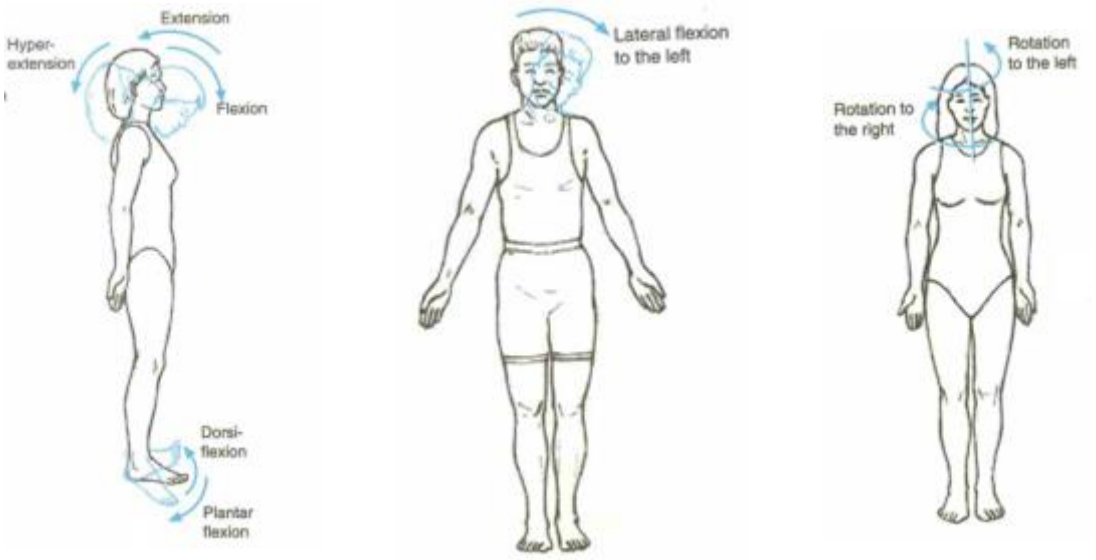

a) b) c)

Figure 2. a)-c) Anatomical terms for motions regarding cervical spine movements (Lowe et al., 2018)

As the human body's longitudinal axis runs through the spine, it defines two directions: *superior* and *inferior*, which points to the head and the heels, respectively. The sagittal plane bisects the body into two parts: *dexter* and *sinister* that is, right and left. Directions defined by the sagittal axis are *anterior* and *posterior*, namely: front and back. When describing a position in frontal plane that is closer to the sagittal plane, one uses the term, *medial*, when farther,

lateral (Szentágothai and Réthelyi, 2006).

Finally, the introduction of anatomical terms of motion follows. *Flexion* occurs about the frontal axis when two adjacent body segments' anterior surfaces approach each other. In case of *extension*, the exact opposite of the aforementioned motion takes place. *Abduction* occurs about the sagittal axis when a specific body part is moved away from the longitudinal axis. *Adduction* is, similarly to flexion/extension motion pairs, the exact opposite motion. *Rotation* includes any twisting motion about the longitudinal axis. Focusing on the neck, all these movements are presented on **Figure 2**.

The fact is worth noting that the pair of terms, abduction and adduction, is not used in relation to neck movements. As it is indicated on **Figure 2.**, *lateral flexion* is used as the official term describing abduction/adduction-like motions, instead.

2.2. ANATOMY OF THE CERVICAL SPINE

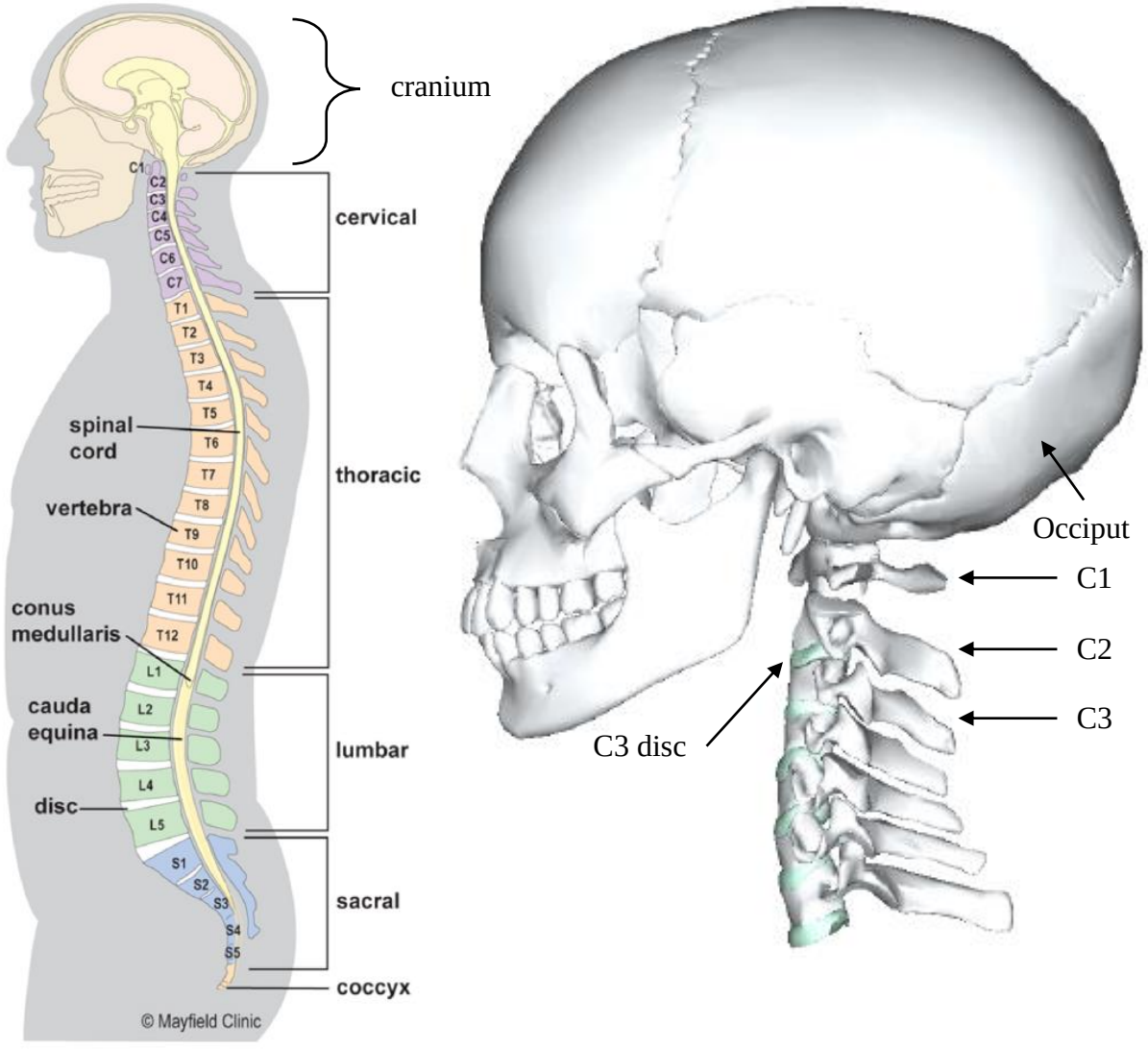

Figure 3. a) Sagittal cross-section of the human body: spinal column (Hines, 2018); b) Lateral view of cervical spine and cranium (Mitsuhashi et al., 2009)

The *spinal column* (**Figure 3.**) is one of the most essential parts of the body with regards

to proper life functioning, which is formed by series of irregular formed bones, called the *vertebrae*. The vertebral column can be divided into 5 parts, out of which the most superior part is called *cervical spine*. The cervical spine consists of 7 vertebrae, which show a few unique features compared to other vertebrae (Gray, 1918). Beside a typical one, the top two vertebrae need special attention due to the specialty of their anatomy and function. Before proceeding in the description of related anatomy, it's worth noting that the rule, by which each vertebrae is commonly denoted, is as follows. Abbreviation consists of the first letter of the name of the spinal column part, which the vertebra in question belongs to, and a number, which indicates the vertebra's position in the concerned spinal column part. For example, C4 refers to the cervical vertebra that is the fourth one, counting from superior to inferior.

On **b)** part of **Figure 3.**, the whole skull and cervical spine can be seen for the sake of generality. Please, note that only the top three vertebra and the skull are taken into account in the finite element model thus these anatomical parts are in the focus of anatomical investigations, too.

For the sake of the present study, a limited description of the human skull is also required, since articulation of the vertebral column with the skull has great importance from a biomechanical point of view.

2.2.1. BONES

Bone is one of the hardest and stiffest tissue in the human body. All of 206 distinct bones' internal structure, which can be observed in an adult human, are nearly the same (**Figure 4.**). The most exterior, thin layer of the bone is called *compact tissue* or *cortical bone*, which appears to be solid but, in fact, is porous. What lies interiorly in the bone is the *cancellous tissue*, also called *trabecular bone* or *spongy bone*. Unlike the other bone tissue, the cancellous bone is visibly porous because of the reticular structure of slender fibers. It's worth noting that the distribution of the two bone tissues among the different bones and even within the same bone is more or less irregular, meaning, for example, that the thickness of the cortical tissue varies along the surface of a vertebra (Gray, 1918).

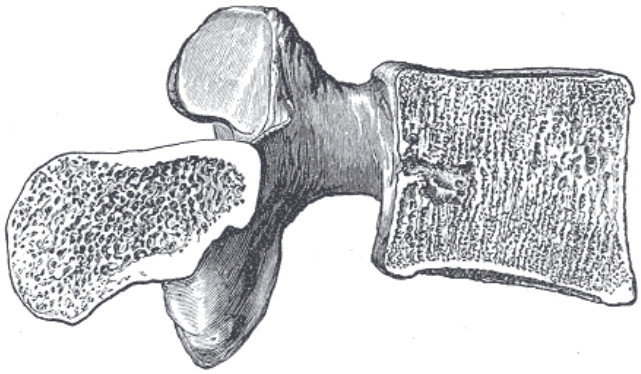

Figure 4. Sagittal cross section of a thoracic vertebra (Gray, 1918)

2.2.1.1. A TYPICAL CERVICAL VERTEBRA

The *vertebral body* is relatively small and is narrower anteroposteriorly than laterally (**Figure 5.**). Its inferior and superior surfaces present some resemblance to parabolic hyperboloids. One can easily imagine that two saddle surface, when one is put onto the other, can hardly be displaced horizontally in a direct way, only vertically: the same occurs to the vertebral bodies.

The *pedicles* project laterally and posteriorly out of the middle of the vertebral body. The *laminae* are narrower and thinner superiorly than inferiorly: they form partly the *vertebral*

foramen, which is large, compared to other vertebrae's, and triangular. The *spinous process* is short and divided into two parts, which are often asymmetric. The *superior* and *inferior articular processes* project laterally from the junction of the pedicle and lamina. Their superior and inferior surfaces are called *articular facets*. The *transverse processes* extend laterally from the vertebral body and encompass the *foramen transversarium*. These processes have an anterior and posterior part, both of which ends in the corresponding *tubercles*. The anterior part of the transverse process is homologue of the rib therefore is commonly called *costal process* or *costal element*. The group of pedicles articular processes and laminae of one vertebra is commonly called *vertebral arch* (Gray, 1918).

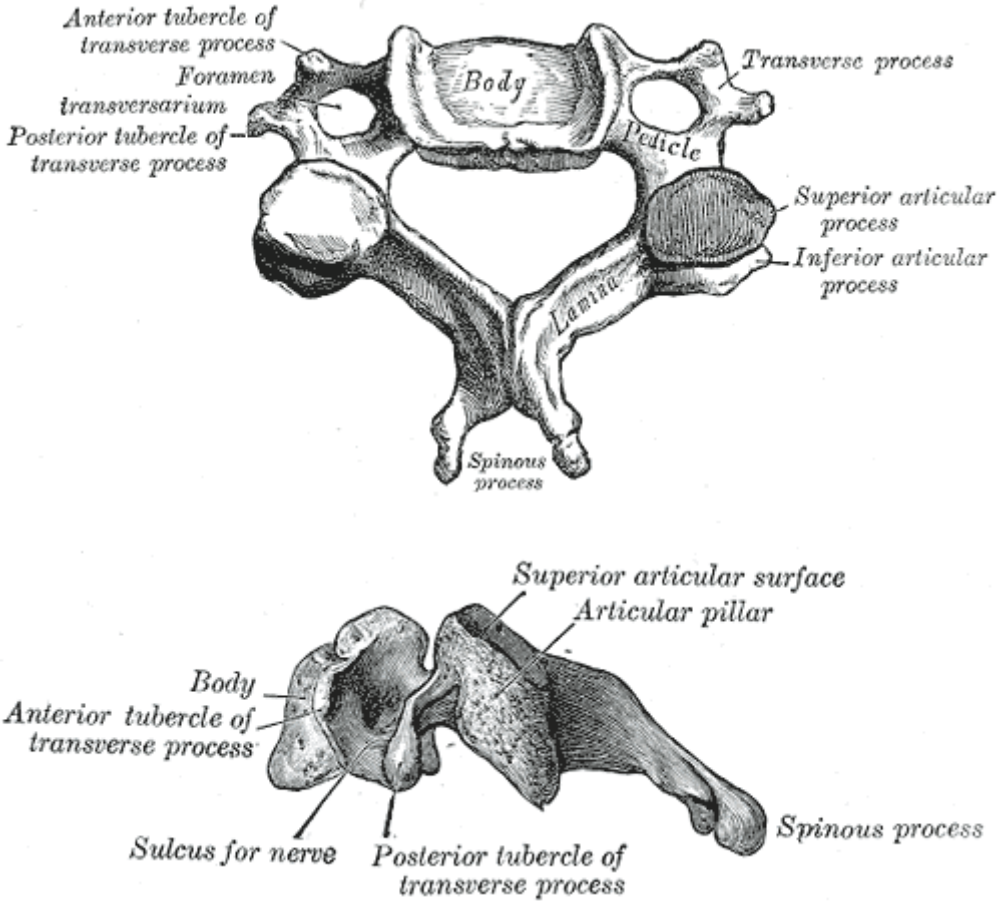

Figure 5. A typical cervical vertebra (Gray, 1918)

2.2.1.2. FIRST CERVICAL VERTEBRA

The first cervical vertebra (**Figure 6.**) has a distinct name: *atlas*. Origin of the name is rooted in Greek mythology: Atlas, who has to hold the sky forever as a punishment, is commonly depicted as if he would hold the globe of the Earth. Similarly, the atlas vertebra holds the globe of the head.

Its main peculiarities are that it has no vertebral body and no spinous process because the former is fused with that of the subjacent vertebra. Instead of the vertebral body and the spinous process, the axis presents the *anterior arch* and *posterior arch*.

The former's anterior surface is convex, on which is located the *anterior tubercle* medially. The anterior arch's posterior surface is concave and is marked by the *fovea dentis*, which provides proper articulation with the subjacent vertebra. The posterior arch forms approximately two-fifths of the ring-like structure of the atlas and, similarly to the anterior arch, it has the *posterior tubercle* medially.

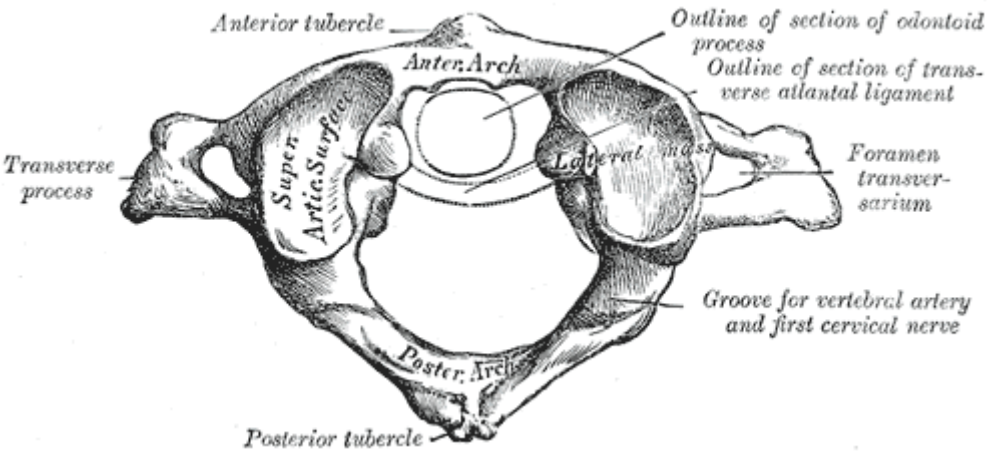

Figure 6. Superior view of atlas (Gray, 1918)

The *lateral masses*, positioning at the junction of the two arches, are the largest and most solid part of the vertebra because mainly the masses serve the role of supporting the head by transmitting axial compressive forces. Similarly to the articular processes, the lateral masses carry two articular facets. The *superior articular facets* are large and form a cup-like surface in order to ensure the proper connection with the *occiput* through the *occipital condyles*. The *inferior articular facets* are somewhat circular and slightly convex thus can articulate with the subjacent vertebra.

On the medial side of the lateral masses, additional tubercles are located, which provide attachment points for ligaments to hold the dens tight. The transverse processes are large and extend laterally from the lateral masses. Their tubercles are fused therefore they can provide massive attachment points for muscles that are responsible for rotation of the head (Gray, 1918).

2.2.1.3. SECOND CERVICAL VERTEBRA

The second cervical vertebra (**Figure 7.**) is called *epistropheus* or, most commonly, *axis* due to its unique anatomy that enables the atlas to rotate. The most apparent feature of the axis is the *odontoid process* or *dens*, which extends superiorly from the vertebral body of the axis.

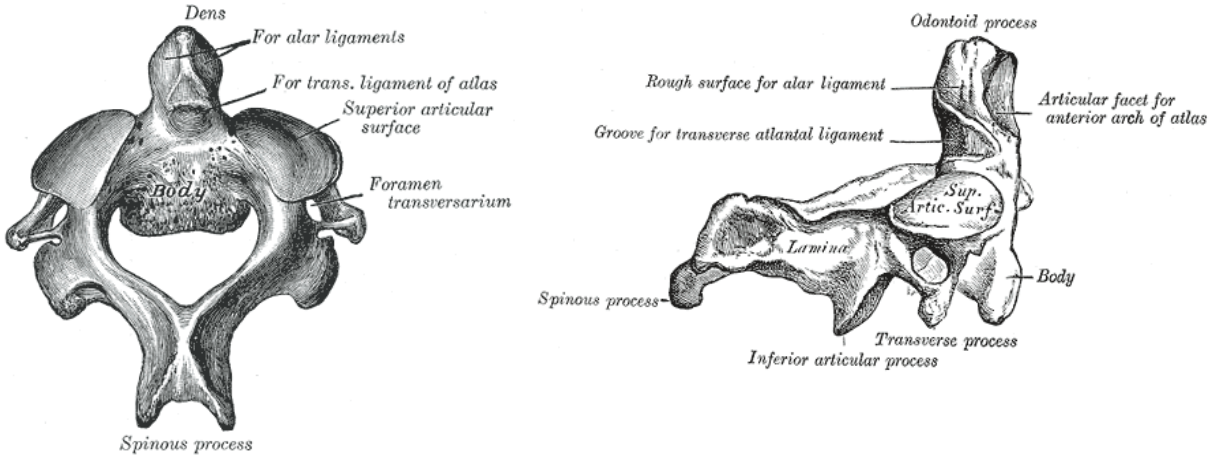

a) b)

Figure 7. a) Superior view of axis (Gray, 1918), b) Lateral view of the axis (Gray, 1918)

Its cross section slightly contracts near the vertebral body. On the anterior side, the dens

has a circular facet for articulating with fovea dentis; on the posterior side, a shallow groove is located, which helps ligaments holding tight the axis.

The *pedicles* are wide and strong and carry the *superior articular facet*. The *laminae* are broad and strong, from which the *inferior articular facet* extends. *Transverse processes* are smaller and are punched through by the *foramen transversarium*. Similarly to the pedicles, the *spinous process* is also large and massive, and exhibits a bifid end with *tubercles* (Gray, 1918).

2.2.1.4. OCCIPITAL BONE

The *skull* is also an essential part of the human body, serving several significant purpose. It can be divided into two parts, each of which is composed of several bones: *cranium*, which protects the brain, and the *skeleton of the face*. Turning our attention to some features of a single bone, the occipital bone, of the cranium is adequate for understanding the present biomechanical problem. The reason why the following parts of the occipital bone is crucial to be presented is that they serve as attachment points to ligaments and muscles related to the cervical spine.

Occipital bone is located posteriorly and inferiorly on the cranium (**Figure 8.**) It's a trapezoidal, curved bone, which is penetrated by the *foramen magnum*. With the help of foramen magnum, four regions of the occipital bone can be defined. *Squama* lies posteriorly, the *basilar part* anteriorly and the *lateral portions* on either side laterally relative to the foramen magnum.

A dominant feature of the squama is the *external occipital protuberance*. From this, four lines extends laterally: superior two are called *highest nuchal lines*, and the inferior two, *superior nuchal lines*. *Median nuchal line* links the external occipital protuberance to the foramen magnum. *Inferior nuchal line* runs laterally on either side from the middle part of the median nuchal line.

On the lateral portions, *condyles* are located closest to the foramen magnum, which articulate with the superior articular facet of the atlas. A tubercle is situated on the medial side of each condyle. An approximately quadrilateral bone, the *jugular process* extends from the lateral side of each condyle.

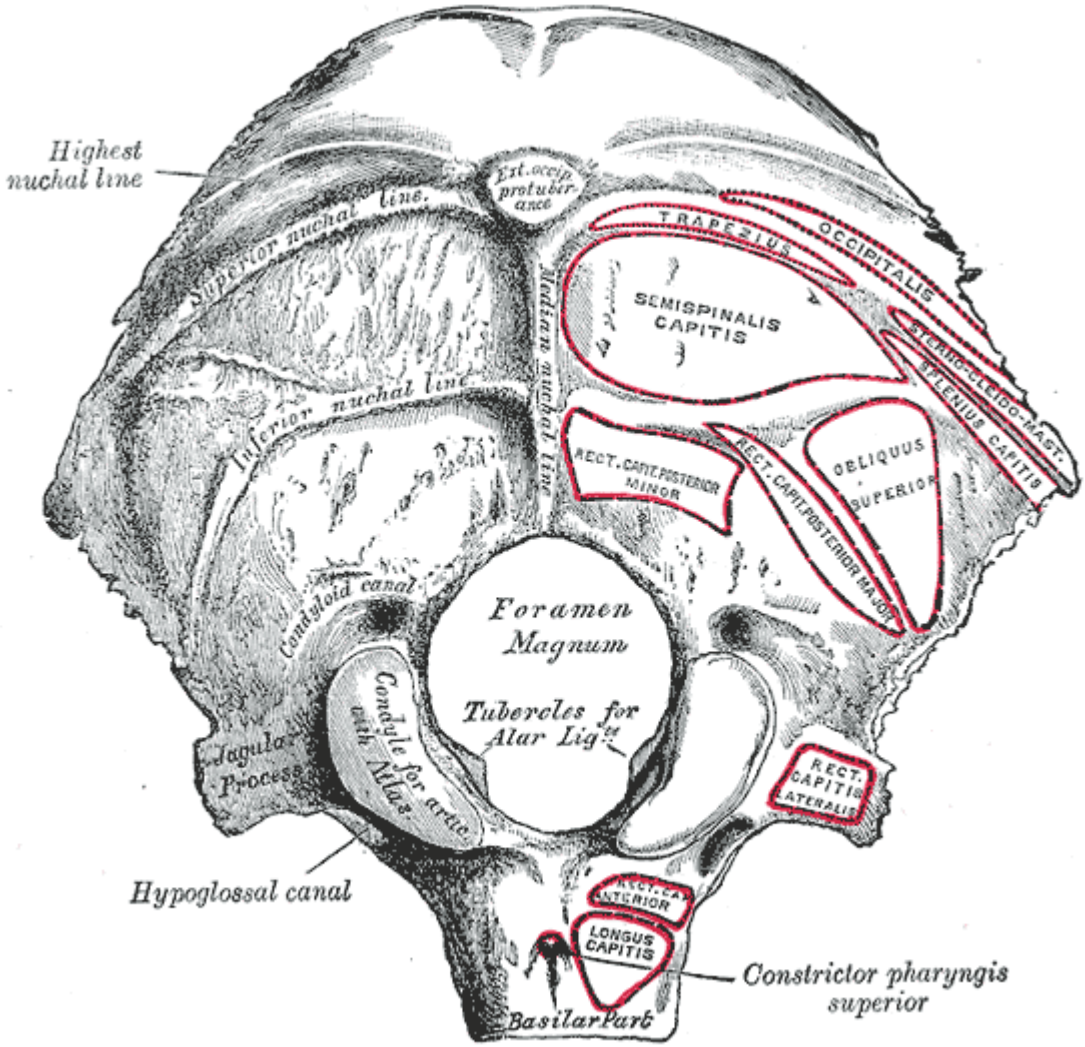

Figure 8. Occipital bone: inferior, outer view (Gray, 1918)

2.2.2. INTERVERTEBRAL DISCS

Intervertebral discs lie between almost every movable vertebra, providing the main connection between adjacent vertebral bodies. The discs' shape, size and thickness vary significantly along the vertebral column. Their shape correspond to the inferior surface of the superior vertebral body and the superior surface of the inferior one thus are saddle surface-like in region of the cervical spine. Additionally, discs between cervical vertebrae have greater thickness anteriorly than posteriorly thus contributing to the cervical curvature. Range of motion in a given spine segment is greatly influenced by the thickness of intervertebral discs in that segment. In the cervical spine, which is the most mobile one, the ratio between thickness of discs and height of vertebrae is larger compared to other spine segments. Intervertebral discs are adherent to the adjacent vertebral bodies by a thin layer of cartilage and to certain neighboring ligaments (Gray, 1918).

The internal structure of each intervertebral disc can be divided into two parts. The circumferential part consists of several layers of fibrous tissue embedded in cartilage: this outer part is called *annulus fibrosus*. The internal section is composed of a soft, pulpy, highly elastic, fluid-like substance, called *nucleus pulposus*. Layers of annulus fibrosus are not straight: outer layers are curved outward, the internal are curved more inward. Also, the fibers, of which each layer in the annulus fibrosus is composed, are directed obliquely; besides, this direction is

inverted in adjacent layers (Gray, 1918).

2.2.3. LIGAMENTS

In addition to intervertebral discs, *ligaments* help forming articulations between bones: they help stabilizing joint, transmitting loads, and restricting motions of joints (Korhonen and Saarakkala, 2011). In the cervical region, they may be divided into four groups with regards to the bones that are connected by these ligaments.

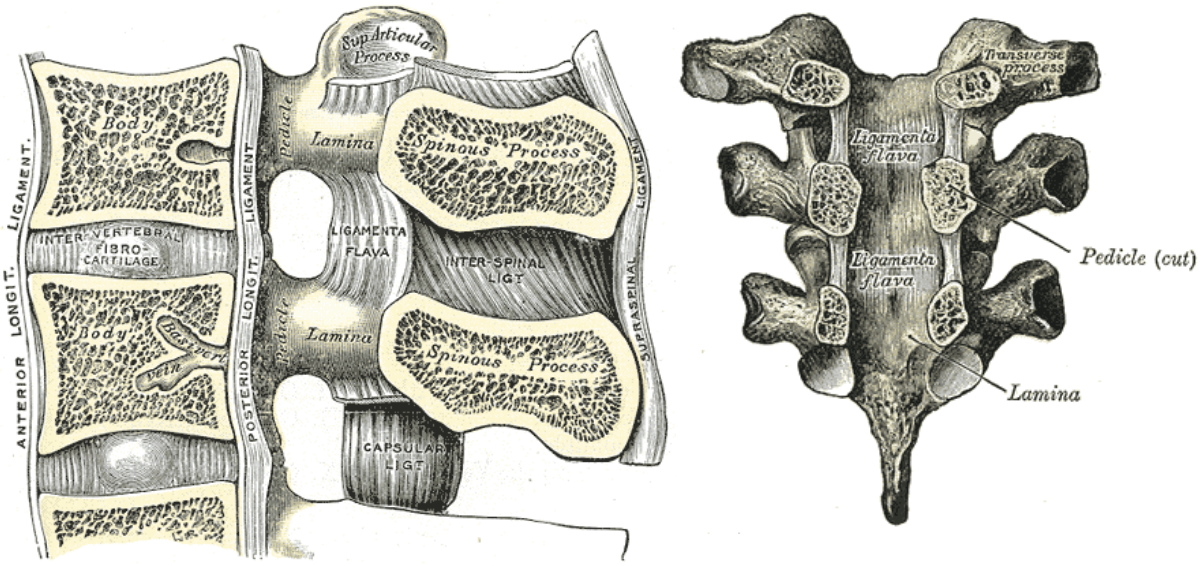

a) b)

Figure 9. a) Median sagittal cross section of the spine: ligaments (Gray, 1918), b) View of ligamentum flavum from the vertebral canal (Gray, 1918)

2.2.3.1. LIGAMENTS OF THE TYPICAL VERTEBRAE

Anterior longitudinal ligament (ALL) extends on multiple vertebral bodies' anterior surface: it starts at the level of axis and ends at the sacrum. It is wider superiorly than inferiorly and is continuous with the anterior atlantoaxial ligament. Along the vertebral column, the anterior longitudinal ligament is more tightly attached to the margins of intervertebral discs and the inferior and superior circumference of the vertebral bodies but is hardly adherent to the middle of the vertebral bodies. In the latter case, the ligament fills the concavities of the vertebral body thus its thickness is larger here. The ligament is composed of layers of fibers, which are closely interlaced but differ in length. The most superficial ones extends through four or five vertebrae. The subjacent layers' fibers spread between only three of four vertebrae and the deepest ones connect two adjacent vertebrae (Gray, 1918).

Posterior longitudinal ligament (PLL) is very similar to the aforementioned one: a main difference is the location of the ligament. As its name suggests, it is situated at the posterior side of several vertebral bodies. Also, it starts at the level of the axis, where it is continuous with the membrane tectoria, and ends at the superior part of the sacrum. Similarly to the anterior longitudinal ligament, it is wider superiorly than inferiorly and is more adherent to the intervertebral discs than to the middle of the vertebral bodies but, at the same time, is thinner at the neighborhood of the discs than of the bodies. As previously, the same amount of layers constitute the posterior longitudinal ligament which have a similar internal structure (Gray, 1918).

Articular capsules or *capsular ligaments* (CL) connect articular processes of adjacent

vertebrae by attaching to their margins. In the cervical spine they are adherent more loosely than in any other spinal region (Gray, 1918).

Ligamentum flavum (LF) connects laminae of neighboring vertebrae, starting from axis and ending with the sacrum. Between adjacent vertebrae, the ligamentum flavum is attached to ipsilateral laminae: it extends from the articular processes to the spinous process. Longitudinally, it is adherent to the anterior margin of the superior lamina and to the posterior margin of the inferior lamina. In the cervical spine, the ligamentum flavum is thin, but broad and long, and its main role is to help sustaining an upright posture and recovering from flexion (Gray, 1918).

Supraspinous ligament (SL) is a strong, thick, and continuous string, which is attached to the apices of the spinous processes of vertebrae, starting from the seventh cervical vertebra to the sacrum. Similarly to the other two longitudinal ligaments, the ligament has a few layers, of which the superficial, the deeper, and the deepest one extends across three or four, two or three, and adjacent vertebrae, respectively (Gray, 1918). SL is not always developed in adult humans (Ivancic et al., 2007).

Ligamentum nuchae (LN) serves a similar role in the cervical spine than the supraspinous ligament in other spinal segments. It is a fibrous membrane, which stretches from the external occipital protuberance and median nuchal line to the spinous process of the seventh cervical vertebra. Its anterior side is connected to the apices of spinous processes of the cervical vertebrae by a thin, fibrous layer. This layer separates contralateral muscles of the neck. Also, this ligament contributes to holding of the neck uprightly (Gray, 1918).

Interspinous ligaments (ISL), which are thin and membranous, are attached to spinous processes of adjoining vertebrae and extends from the root to the apex of each spinous process. In other words, interspinous ligaments touch ligamentum flavum at their posterior side, and supraspinous ligaments at their anterior side. In the cervical spine, this ligament is slightly developed (Gray, 1918). ISL is not always developed in adult humans (Ivancic et al., 2007).

Intertransverse ligaments (ITL) are stretched between transverse processes of neighboring vertebral bodies. In the cervical region, these ligaments consists of only a few, weak fibers thus don't have as much significance as in other regions of the vertebral column (Gray, 1918).

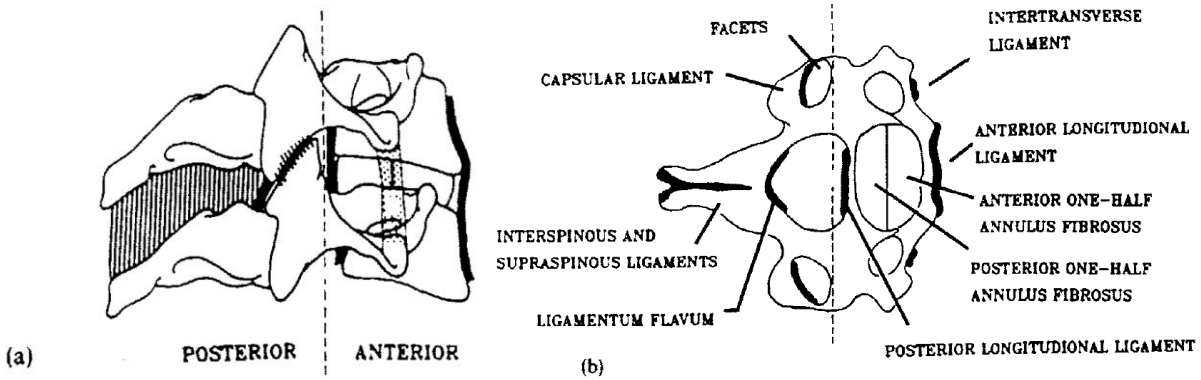

Figure 10. (a) and (b) Overview of ligaments of a typical cervical vertebrae (Goel et al., 1984)

2.2.3.2. LIGAMENTS OF THE ATLANTOAXIAL ARTICULATION

Atlantoaxial articulation refers to the ensemble of the atlas, the axis and related ligaments. Since these two vertebrae has a special anatomy, the connecting ligaments adapt to the specialty thus further attention is necessary.

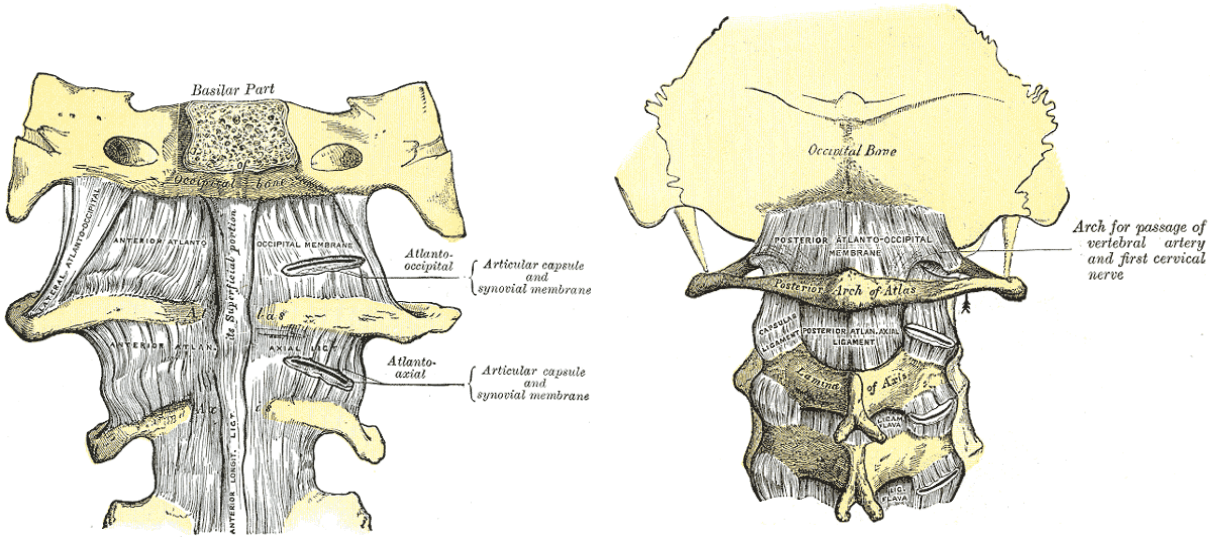

Figure 11. a) Anterior view of atlantooccipital articulation (Gray, 1918), b) Posterior view of atlantooccipital articulation (Gray, 1918)

Capsular ligaments (CL) are thin and loose fibers between the lateral masses of the atlas and the articular processes of the axis. Each is reinforced posteriorly and medially by an accessory ligament, which extends from the base of the odontoid process to the lateral masses.

Anterior atlantoaxial ligament (AAL) is a strong membrane, which links the inferior margin of the anterior arch of the atlas to the anterior surface of the axis. The continuation of the anterior longitudinal ligament strengthens the membrane medially, and it is attached to the tubercle of the anterior arch of the atlas as well as to the body of the axis (Gray, 1918).

Posterior atlantoaxial ligament (PAL) is a thin membrane: its superior and inferior end is attached to the inferior edge of the posterior arch of the atlas and to superior border of the laminae of the axis, respectively. This ligament substitutes the ligamentum flavum in the atlantoaxial articulation (Gray, 1918).

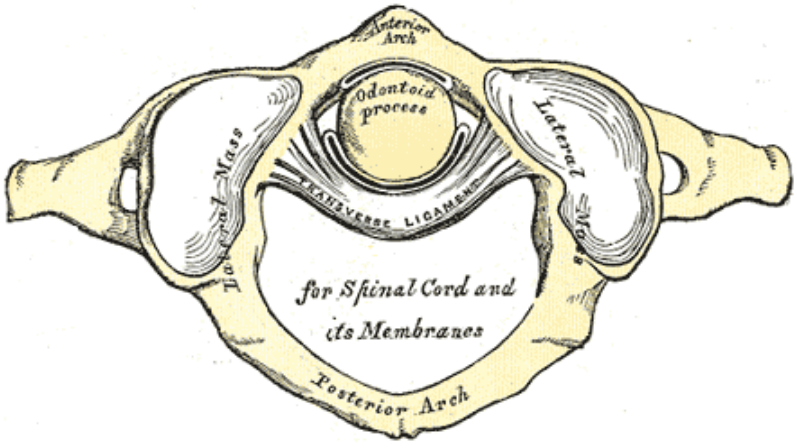

Figure 12. Superior view of the atlas with the transverse ligament (Gray, 1918)

Transverse ligament of the atlas, or *transverse ligament* (TL) is wide and strong, which also serves the role of holding the atlas and the axis tight together through the odontoid process. The two main attachment points of the transverse ligament are the tubercles of the lateral masses of the axis. The ligament becomes wider and thicker close to the odontoid process and narrower

close to the tubercles. When passing the odontoid process, two fiber bundle expands longitudinally from the most superficial layer, which is the most posterior, of the transverse ligament. The one that is attached to the basilar part of the occipital bone is called *crus superius*, and the other, which extends to the posterior surface of the vertebral body of the axis, crus inferius. The two together constitute the *cruciate ligament of the atlas* (Gray, 1918).

Synovial membranes.

2.2.3.3. LIGAMENTS OF THE ATLANTOOCCIPITAL ARTICULATION

Capsular ligaments (CL) connect the condyles of the occipital bone with the articular processes of the atlas; they are thin and loose.

Anterior atlantooccipitial membrane (AAOM) is a wide ligament, consisting of densely interlaced fibers, which extends from the anterior edge of the foramen magnum to the superior edge of the anterior arch of the atlas. Besides, a strong cord of fibers runs from the tubercle of the anterior arch of the atlas to the basilar part of the occipital bone.

Posterior atlantooccipital membrane (PAOM), which is wide, too, but thin, stretches from the posterior edge of the foramen magnum to the superior margin of the posterior arch of the atlas.

Lateral ligaments (LL) are connected to the jugular processes of the occipital bone and to the bases of the transverse processes of the atlas. These ligaments are the strengthened parts of the articular capsules.

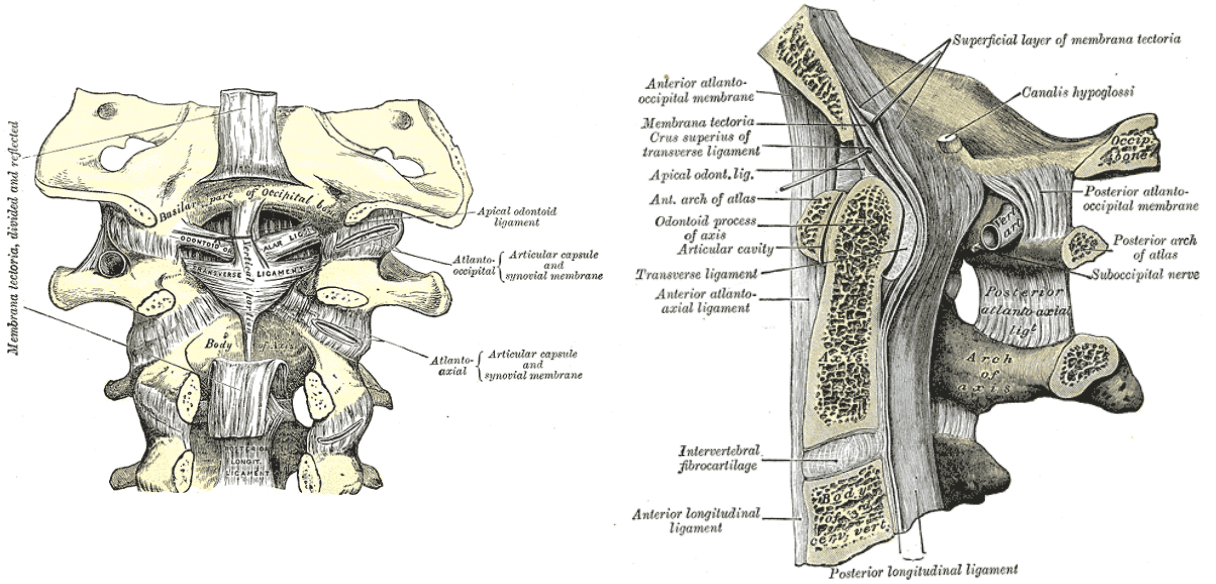

a b

Figure 13. a) Posterior cross section the the atlantooccipital articulation (Gray, 1918), b) Median sagittal cross section of the occipital bone and the first three cervical vertebrae (Gray, 1918)

2.2.3.4. LIGAMENTS CONNECTING THE AXIS WITH THE OCCIPUT

Tectorial membrane (TM) is wide and strong band of fibers, which, practically, is the continuation of the posterior longitudinal ligament. Its inferior end is fixed to the posterior surface of the vertebral body of the axis and its superior end is adherent to basilar groove, close to the anterior margin of the foramen magnum.

Alar ligaments (AL) are two strong truss, stretching from the apex of the odontoid process laterally to the condyles of the occipital bone close to the foramen magnum. Additionally, the

apical odontoid ligament, too, arises from the superior border of the odontoid process but runs medially to the anterior edge of the foramen magnum. The latter ligament virtually blends into the anterior atlantooccipital membrane and the superior crus of the transverse ligament. Also, alar ligaments contribute to the limitation of rotation of the cranium.

2.2.4. MUSCLES

In general, the muscular system is responsible for the movement of the human body. This system is composed of about 700 distinct muscles, which are attached to various skeletal parts. Three type of muscle tissues can be distinguished: *visceral*, *cardiac* and *skeletal* (Barclay, 2019). From a biomechanics point of view, only skeletal muscles are of interest since they affect neck injury therefore the other two forms of muscle tissue are not discussed here.

Skeletal muscles are the only ones that allow voluntary body motion, which is produced by contraction of the muscles. When in contraction, muscles move two bones, which they are attached to, closer to each other. This bone-muscle-bone connection is formed by *tendons* or *aponeuroses*, which are composed of tough bands of connective tissue capable of resisting large tensile forces (Barclay, 2019).

The whole muscle is covered and divided by different connective tissues (**Figure 14.**). The exterior one that holds together the entire muscle is called *epimysium*. The epimysium enwraps bundles of fibers, which are enclosed by the *perimysium*. Finally, *endomysium* is responsible for attaching individual fibers in one bundle together. A *muscle fiber* is composed of a contractile substance and a tubular sheath, which is called *sarcolemma*. These fibers are most commonly prismatic, tubular and may be rather long: up to 30 cm (Betts et al., 2013).

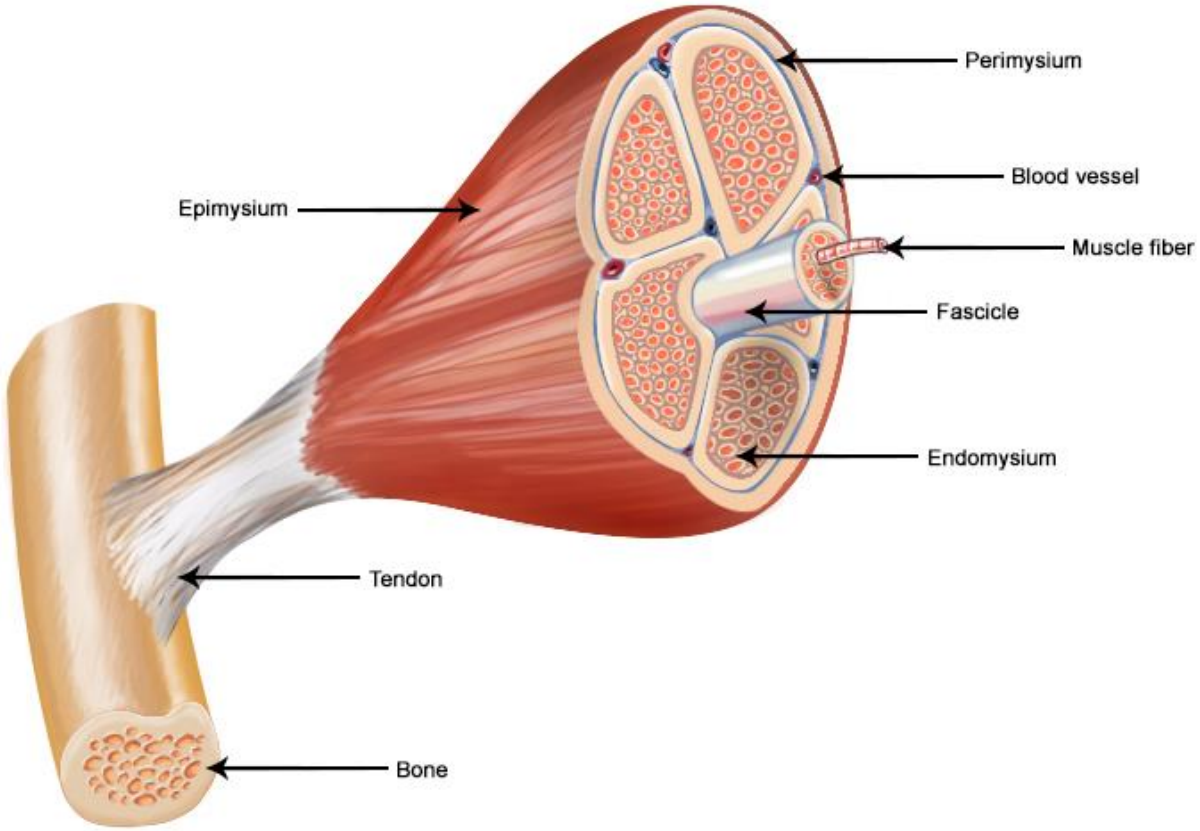

Figure 14. Structure of skeletal muscle ("Structure of Skeletal Muscle," n.d.)

Muscles in the cervical region are numerous, compared to ligaments, and serve several purposes, not to mention the fact that many muscles of the back has attachment points on the

cervical spine and the skull thus they also contribute to the motion of the head. On **Figure 15.**, those muscles are named and shown that play an important role in stabilizing the head or the cervical spine.

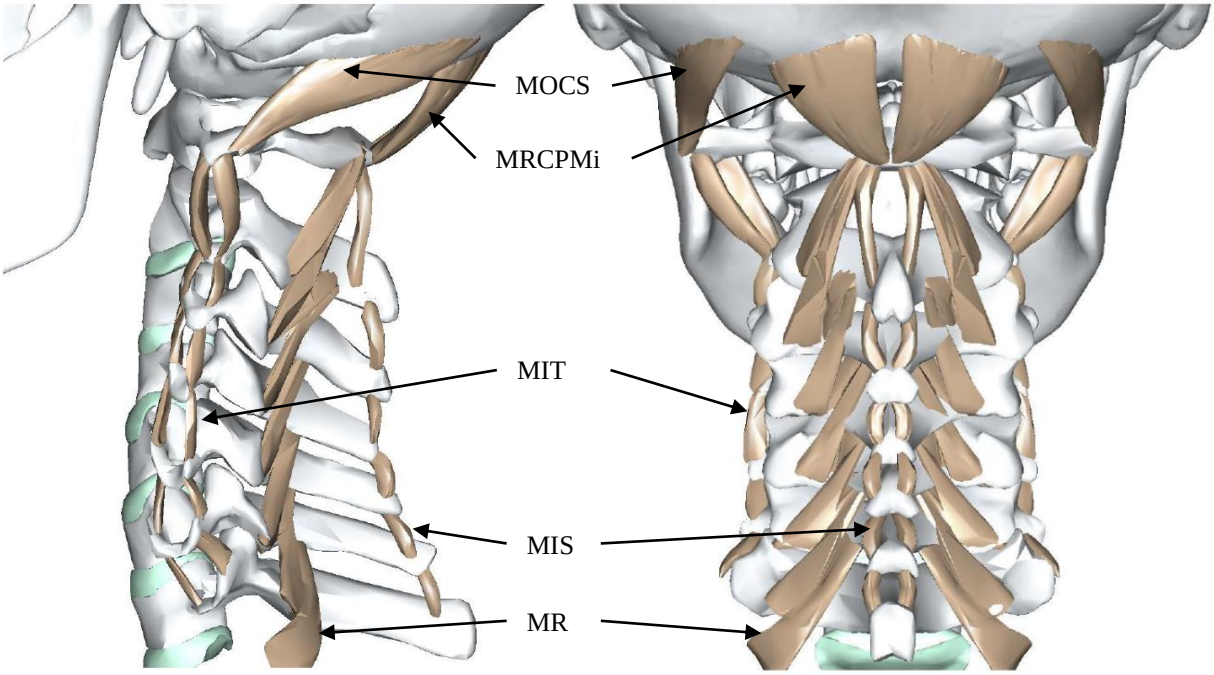

Figure 15. Muscles and muscle groups that are modelled (Mitsuhashi et al., 2009)

3. BIOMECHANICAL ANALYSIS OF THE CERVICAL SPINE

3.1. MATERIAL CHARACTERISTICS OF CERVICAL TISSUES

Reviews on different material modelling approaches with regards to human soft tissues: Freutel et al., 2014 Korhonen and Saarakkala, 2011.

In general, two of the most predominant properties of biological materials are anisotropy and heterogeneity. Additionally, most tissues present viscoelastic behavior: consequently, their response is time- and history-dependent as well as elastic (Pal, 2014).

3.1.1. BONES

Both fluid and solid phases constitute the bone material. Solid phase can be separated into organic and inorganic phase, each of which contributes to uniquely to the overall behavior of bone. Namely, organic material gives the bone its flexibility while the inorganic one provides high ultimate strength and stiffness (Pal, 2014).

As it was mentioned in **Bones** previously, two main structural section can be distinguished in the material: cortical and cancellous. The material components of the two tissue are identical, the only difference between them is their porosity. The cancellous tissue's structure adapts to the external loads so that the forces are resisted using the least amount of material. This remarkable adaptation is not only load-, but time dependent, too. Therefore most of the high degree of anisotropy and heterogeneity of the cancellous bone stems from the bone's capability to change its inner structure in the aforementioned way. On the contrary, cortical bone tissue may be regarded as linearly elastic, transversely isotropic and homogenous (Pal, 2014; Oftadeh et al., 2015).

The bone, as a whole, may reach a short plastic state before failure (**Figure 16.**) (Bankoff, 2012). On the other hand, cortical bone tissue exhibits significant plastic behavior in tension as well as in compression (Natali and Meroi, 1989). Additionally, the bone is highly strain-rate

sensitive, but not under physiologic conditions (Pugh et al., 1973), meaning that the more the velocity of strain is, the more stiff the bone become (**Figure 16.**) Also, the mechanical properties of the cortical and cancellous bone differs considerably. The former is much stiffer, more rigid thus less capable of shock-absorption Pal, 2014.

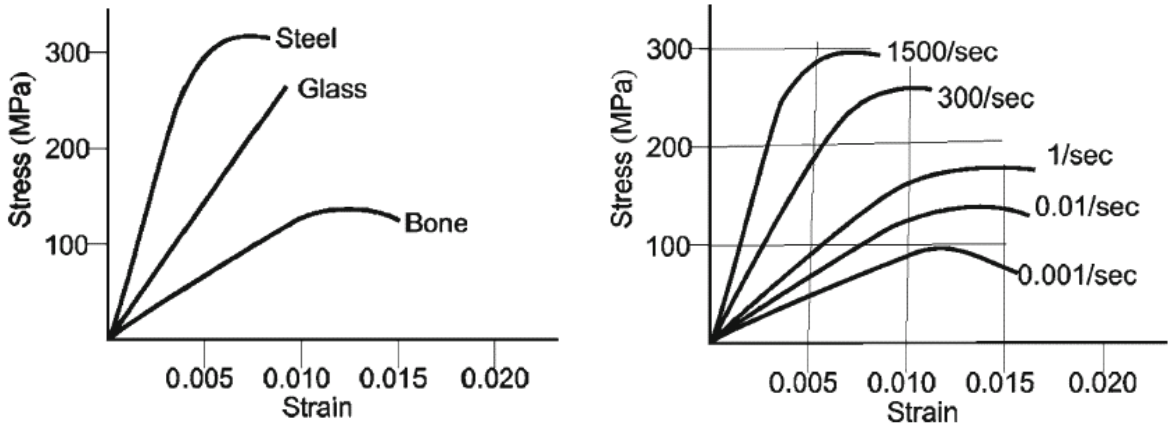

Figure 16. a) Stress-strain curve of bone tissue and other materials for comparative purposes (Pal, 2014) b) Strain-rate behavior of the bone (Pal, 2014)

Bone stiffness, density, ultimate strength, ultimate strain Pal, 2014

3.1.2. LIGAMENTS

Ligaments are composed of biphasic materials, namely: fluid and solid, therefore have a highly viscoelastic behavior (Korhonen and Saarakkala, 2011). Ligaments' fully nonlinear viscoelastic nature was shown to minimize muscles' effort to maintain posture and, at the same time, maximizes stability under dynamic conditions (Troyer and Puttlitz, 2012), which is the reason why taking viscoelastic features into account would be essential to model human ligaments.

Numerous attempt was made to determine characteristic material properties of the human ligaments. The approach of most of these attempts can be classified into two categories. One approach is to measure force-displacement relationship with single or multiple constant loading rate (Ivancic et al., 2007; Mattucci et al., 2012, 2013; Trajkovski et al., 2014a; b) and the other is to measure viscous properties, which are independent of loading rate (Weiss et al., 2002; Lucas et al., 2008; Troyer and Puttlitz, 2011, 2012). Ligament geometric, failure, and stiffness data are also reported (Yoganandan et al., 2000, 2001; Mattucci et al., 2012).

Chazal et al., 1985 determined the quasi-static force-displacement curve of ligaments at several spinal levels and reported on the general behavior of the ligaments, namely: the force-displacement curve can be separated into three parts: a concave, a linear, and a convex part. Among others, the authors concluded that there's not much difference between the same type of ligaments of different spinal levels thus their findings are applicable to the analysis of cervical spine. They also note that intertransverse, posterior longitudinal ligament and ligamentum flavum were the most resistant.

Mattucci and Cronin, 2015 determined the representative force-displacement curves for most of the cervical spinal ligaments for three different strain rates based on previously acquired data.

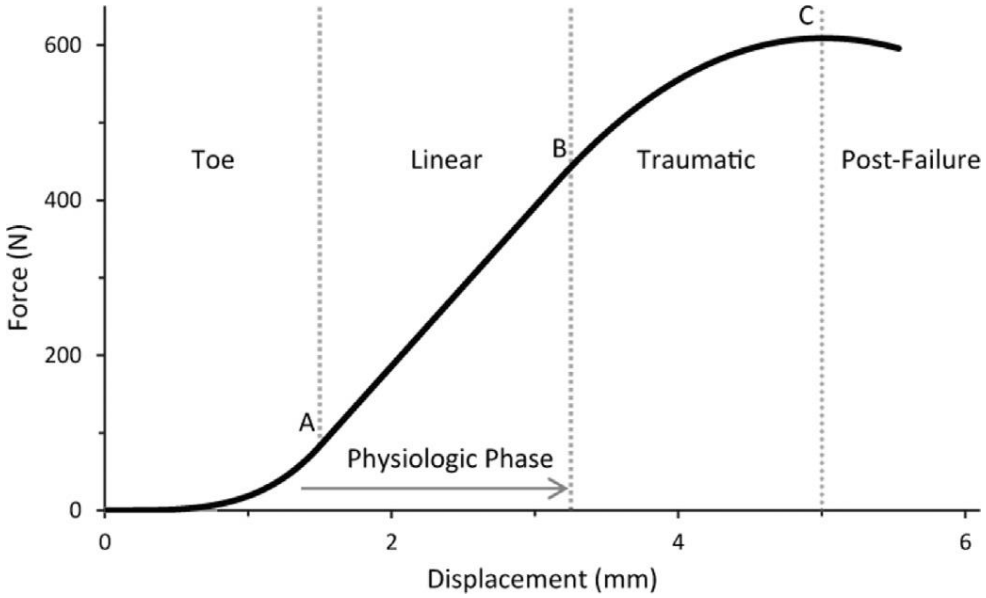

Figure 17. Quasi-static idealized stress-strain curve of ligaments (Mattucci and Cronin, 2015)

3.1.3. MUSCLES

Muscles are a special kind of tissue with regards to their ability to exert forces by contracting. This property of the muscle tissue further complicates material modeling since the mechanical behavior is dependent on the activation level. Based on this concept, at least two muscle activation state can be distinguished: *active* and *passive*.

When muscles are in passive state, no excitation signal is transmitted by the nerves thus no force is generated. Reviewing on passive muscle tensile properties, a clear convergence of the findings can be seen: an exponential-like force-displacement relationship seems to be the best fit (Hedenstierna, 2008) (**Figure 18.**).

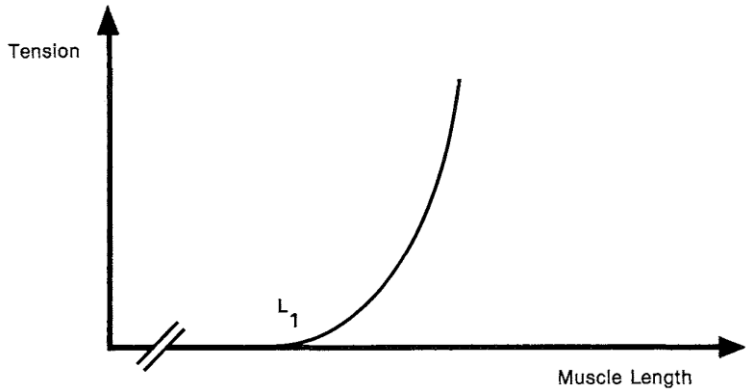

Figure 18. Idealized force-displacement curve of passive muscles (Herbert, 1988)

On the other hand, when in active state, muscles are excited by the nerves to contract. There are several factors that affect the maximum generated force by the muscle tissue; these are: *muscle size*, *muscle fiber angle*, *physiological cross-sectional area* (PCSA), and *optimal muscle length* (Hedenstierna, 2008).

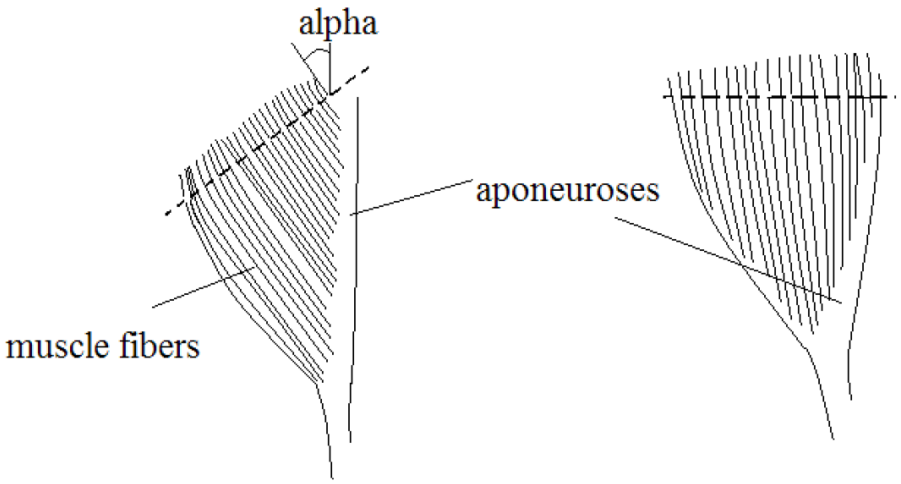

Figure 19. Concept of muscle fiber angle (Hedenstierna, 2008)

Muscle fiber angle may be varied relative to the line of action of the force that is generated by the muscle in question (**Figure 19.**) The concept of PCSA is strongly connected: it is the cross-sectional area of the muscle fibers perpendicular to the fiber direction. The produced maximal force is also dependent on the relative length of the muscle. This relative length is described as the ratio of the current length and the rest length. When the muscle reaches its optimal length, the force inducing capacity is at its maximum (Pandy and Barr, 2004; Panzer, 2006; Hedenstierna, 2008). Active and passive kinetic properties of the muscle is summarized on **Figure 20**.

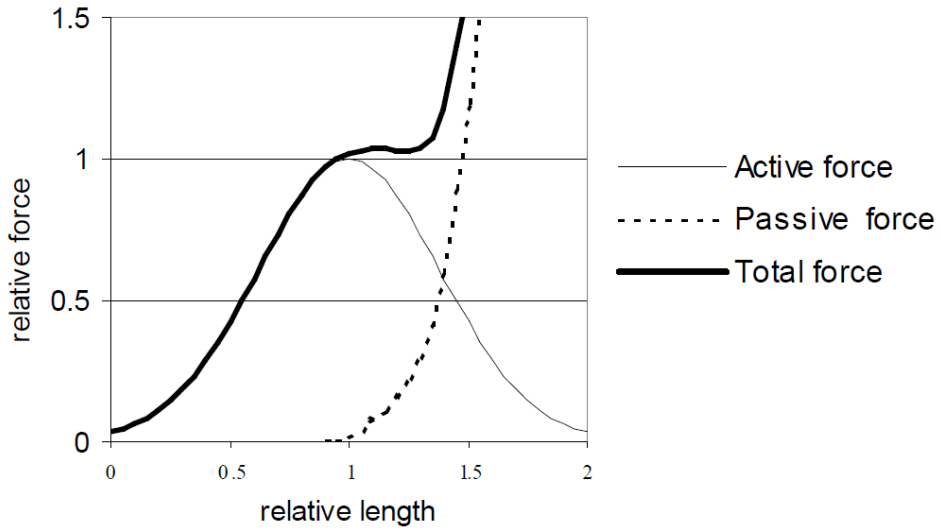

Figure 20. Total force produced by muscle tissue with respect to its relative length (Hedenstierna, 2008)

One of the most widely used muscle model originates from the work of Hill, 1938 (**Figure 21.**). His discrete model is composed of a Contractile Element (CE), which generates force if activation signal is present; a Parallel Element (PE), which represents the viscoelastic behavior of connective tissues of epimysium, perimysium and endomysium; a Series Element (SE), which accounts for the tendons. The muscle mass (M) is also taken into consideration (Jovanović et al., 2015).

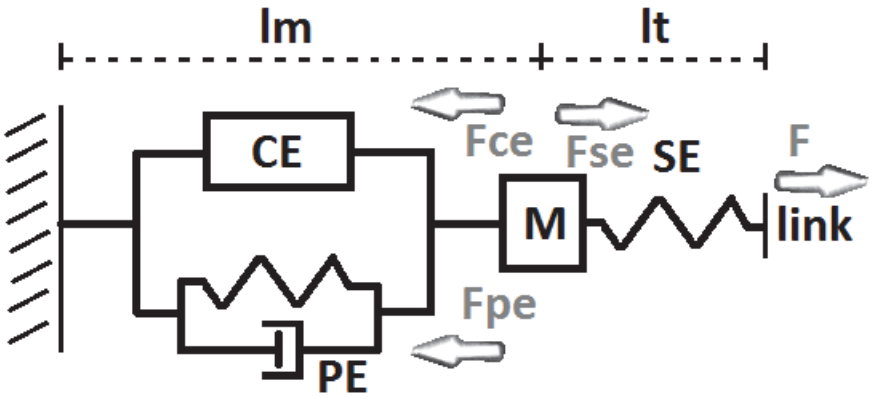

Figure 21. Representation of Hill's muscle model (Jovanović et al., 2015)

From an injury mechanics perspective, the following categorization of the muscles may be useful: one can distinguish *stabilizer* or *mover muscles*. The former are mainly short and, as the name suggest, responsible for stabilizing the posture of the body. Consequently, these muscles are in active state for a longer period of time. In the cervical region, the deep muscles are responsible for maintaining posture (Chancey et al., 2003). While mover muscles facilitate the change of the posture thus they can enable great range of motion. Hence, these muscles, on average, are activated to a lesser degree and for a shorter period of time compared to stabilizer muscles.

In a review, the activation time of the muscles in humans are showed to be substantially greater as opposed to the time under which injury occurs (Hedenstierna, 2008). This fact means that the protective effect of contraction of mover muscles may be ignored when modelling a real life accident.

3.1.4. INTERVERTEBRAL DISCS

The intervertebral discs structure is well adapted to transferring compressive axial forces between adjacent vertebral bodies (**Figure 22.**) Overall, the behavior of the intervertebral disc bears resemblance to that of ball joints.

Nucleus pulposus has a very high water content that ensures the capability of being in hydrostatic pressure state when acted upon by compressive axial forces (Wagner and Lotz, 2004; Newell et al., 2017).

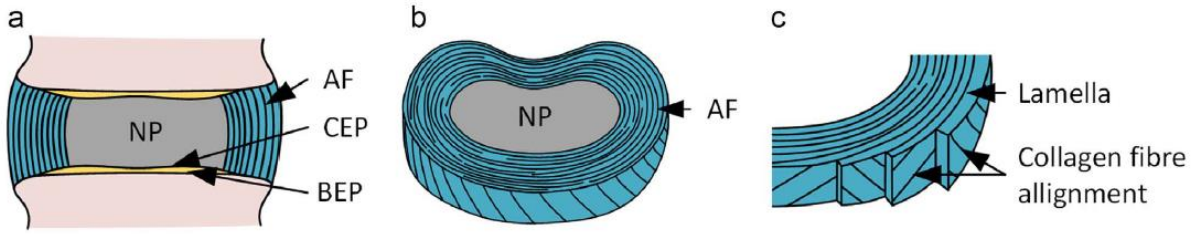

Figure 22. (a) Coronal section of intervertebral disc. (b) View of a transversely sliced intervertebral dis., (c) Alternating fiber alignment in annulus fibrosus between adjacent layers. (Newell et al., 2017)

The oblique arrangement of the annulus fibrous layers are optimal to resist tensile forces, which may arise from nucleus pulposus under hydrostatic pressure state, or bending or rotation of the spine. Therefore it not only serves as a wall of the nucleus pulposus but also connect two adjacent vertebral body very similarly as ligaments (Wagner and Lotz, 2004; Kurutz, 2010).

3.1.5. ARTICULAR CARTILAGE

Articular cartilage is a connective tissue that can be found on the ends of bones, enabling diarthrodial joints to function properly. In humans, the thickness of cartilage is between 1-6 mm. Like bone, articular cartilage is also composed of a fluid and solid phase: the chief constituent of the former is water while the main components of the latter are fibrils (Korhonen and Saarakkala, 2011; Landínez-Parra et al., 2012; Pal, 2014).

When acted upon by compressive forces at least for a minute, the fluid phase flows out of the tissue but with decreasing magnitude with respect to time. This nonlinear fluid flow, which is also responsible for the highly viscous behavior, enable the cartilage to absorb shock of external loads. However, for shorter periods of time, say 1 to 5 seconds, articular cartilage exhibits mostly linear elastic mechanical response. Also, another similarity between bone and cartilage is the capability of adapting to external loads and other demands of body. Additionally, the inner structure of the articular cartilage is not uniform. It can be divided into four zones: superficial, middle, deep, calcified zone (Pandy and Barr, 2004; Korhonen and Saarakkala, 2011; Landínez-Parra et al., 2012; Pal, 2014) (**Figure 23.**)

Due to its different zones and components, articular cartilage is very well adapted to resisting compressive forces and facilitating gliding (Pal, 2014).

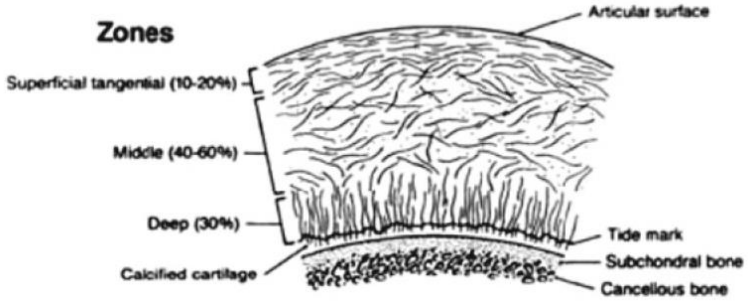

Figure 23. Inner structure of articular cartilage (Pal, 2014)

3.2. BIOMECHANICS OF THE CERVICAL SPINE

The cervical spine is one of the structure of the body that has utmost importance. It supports the head; it allows the head to move flexibly, compared to other spinal segments, to scan the environment; and it also protects the spinal cord. To highlight the valuable service of the cervical spine, note that any injury to the spinal cord could result in some form of disability but invariably cause death if the damage occur at the level of C3 or above. The reason for this is because nerve signals controlling heart and respiratory function would be disrupted in the aforementioned situation (King, 2018a).

Overall, the spine in general is best understood as a column that has slightly deformable masses (vertebrae) connected to each other by viscoelastic structures, which are the ligaments, muscles and intervertebral discs (Nightingale et al., 2015).

3.2.1. NORMAL KINEMATICS OF CERVICAL SPINE

Regarding motions, the cervical spine can be separated into three segments, each of which has a unique anatomy thus unique function. These segments are the aforementioned atlas, axis and typical vertebrae. First, normal functioning of these three portions of the cervical spine need to be understood in order to be capable of properly apprehending injury mechanisms.

3.2.1.1. ATLAS

As noted before, the atlas plays the role of connecting the head, through the occipital

condyles, to the vertebral column. It receives the convex condyles into its concave, deep superior articular sockets thereby allowing only nodding movement between the cranium and the atlas. In all other regards, these two structures behave as one unit: the chief constraint on other motions of the atlanto-occipital joint is the articular capsule (Bogduk and Mercer, 2000).

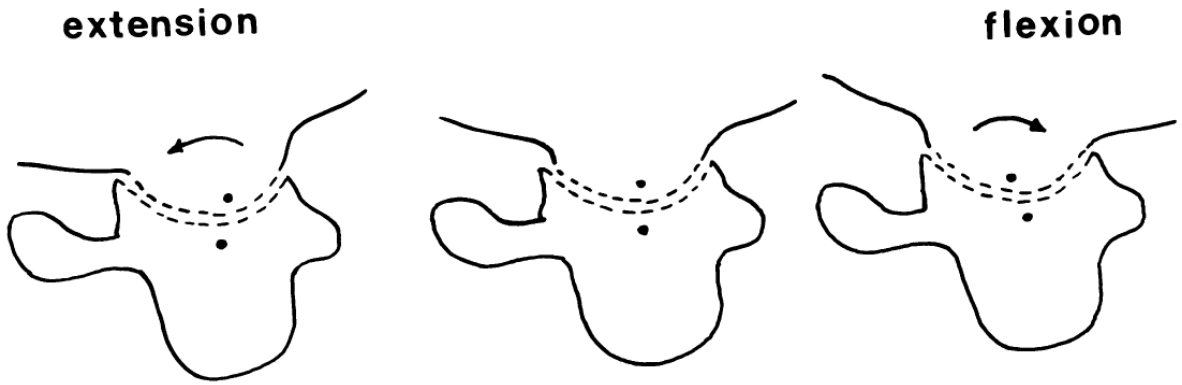

Figure 24. Right lateral view of the atlanto-occipital joint in extension and flexion (Bogduk and Mercer, 2000)

When in flexion, the occipital condyles roll anteriorly in their sockets and, simultaneously, glide posteriorly due to the mass of the head and the respective muscles (**Figure 24.**) In extension, the exact opposite types of motions take place. Flexion or extension motion of the atlas is not limited by any ligamentous structure, instead, it freely moves until the posterior arch hits either the occiput or the C2, respectively. Axial rotation is constrained by the alar ligaments and the articular capsules. The latter ones' contribution to restraining rotation is minor compared to the alar ligaments. Posterior sliding of the atlas is hindered solely by the impaction of the anterior arch to the odontoid process while there's no bony obstacle when sliding anteriorly: this movement is limited by the transverse ligament (Bogduk and Mercer, 2000; Clark et al., 2011).

3.2.1.2. Axis

The primary two function of the axis is to support the atlas and to allow large range of rotation with the help of the odontoid process. The axial rotation of the atlas necessitates the gliding of the anterior arch around the dens and the opposite directional sliding of the lateral masses on the superior articular facets of the axis (**Figure 25.**) Due to the convexities of the joining facets, as the atlas rotates, it descends down on the articular facet of the axis (**Figure 26.**) (Bogduk and Mercer, 2000).

The motions permitted by the axis are primarily constrained by ligaments, e.g., axial rotation is limited chiefly by the alar ligaments. To highlight how fitting the nickname of the C2 vertebra is, it accounts for 77% of axial rotation in the cervical spine. The ability of allowing flexion and extension motion is also present at the level of axis. These movements are restricted by cruciate ligament, and articular facets and tectorial membrane, respectively (Chen et al., 2011).

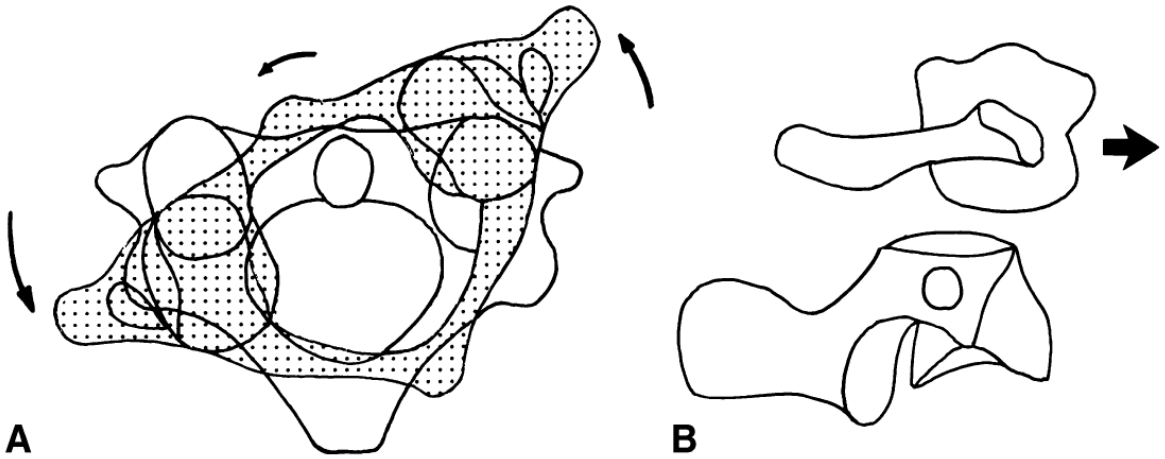

Figure 25. Axial rotation of the axis. a) Superior view b) Right lateral view (Bogduk and Mercer, 2000)

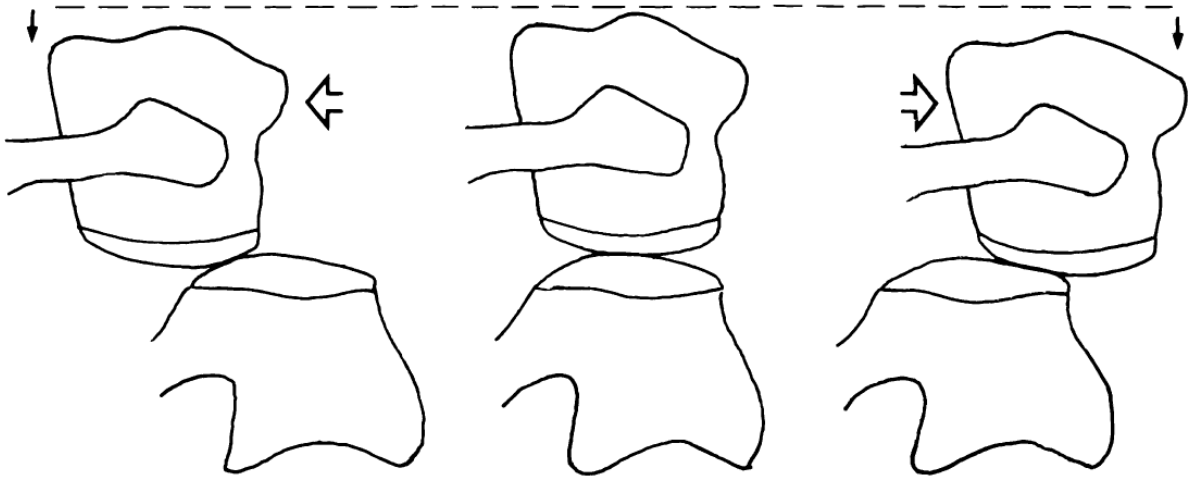

Figure 26. Right lateral view of the atlanto-axial joint and the its components' motions due to the biconvex shape of the articular facets (Bogduk and Mercer, 2000).

3.2.1.3. TYPICAL VERTEBRAE

Rest of the cervical spine is formed by similarly shaped vertebrae, which are considered as typical. As noted in **Chapter 2.2.1.1**, the superior and inferior surface of normal cervical vertebral bodies bear a great resemblance to mathematical saddle surfaces. In addition, these surfaces are curved in a way that primarily facilitates flexion/extension movements and secondarily lateral flexion motions. Due to the aforementioned feature of the vertebral bodies and the position of the articular processes, two axes of pure rotation are directed obliquely relative to the vertical axis (**Figure 27.**) This inclination of the three axes results in a coupled movement of the individual vertebra. For instance, when the whole neck either rotates horizontally or flexes laterally, so do each vertebra both of the cases. Another consequence of the motion patterns of the vertebrae is the structure of the intervertebral discs that are located in between. The annulus fibrosus of these discs are not annular, contrary to the terminology (**Figure 27.**) Merely the anterior side of the vertebral bodies are connected to each other by fibers (Bogduk and Mercer, 2000).

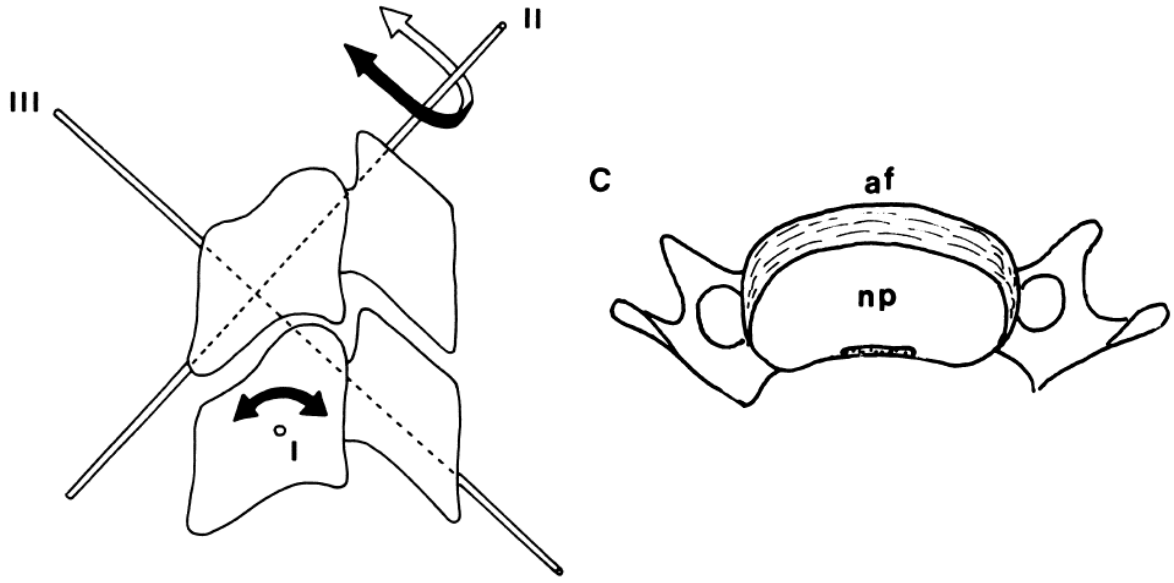

Figure 27. a) Pure axes of rotation of a typical cervical vertebra b) Structure of intervertebral disc of a typical vertebra (Bogduk and Mercer, 2000)

3.3. IMPACT INJURY MECHANISMS

In the present study, the investigation of the injury mechanisms and resulting injuries are not carried out. However, a preliminary summary is still presented in the following paragraphs in preparation for later FEM analysis.

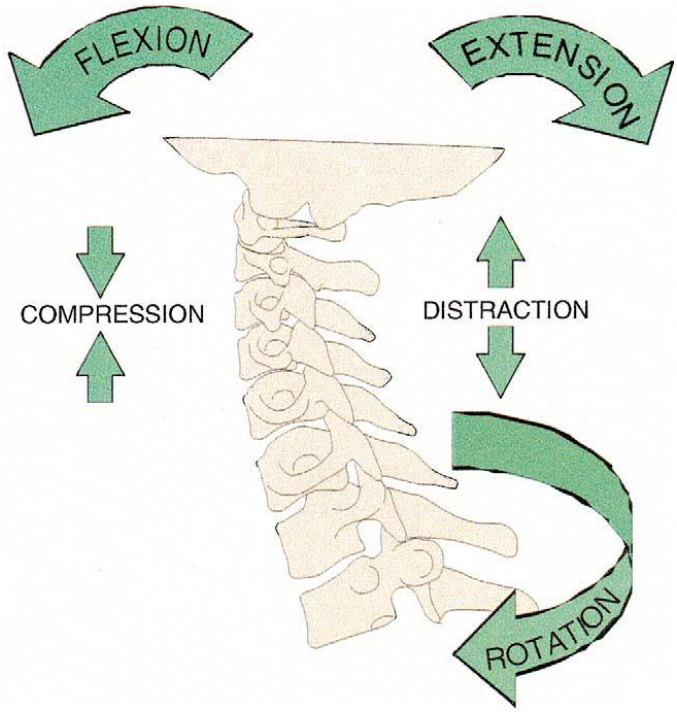

Figure 28. Illustration of different forces acting on the cervical spine (Cusick and Yoganandan, 2002)

There are several cases when cervical spinal injuries can occur, such as motor vehicle crashes and various sport activities, for instance football, ice hockey, rugby, snowboarding, skiing, and diving (King, 2018b), which all can cause either *soft tissue* or *hard tissue injury*. In the former case, any tissue may suffer damage, other than the bone tissue, which consequently

means that soft tissue injuries are mild ones. On the other hand, hard tissue injuries involve harm to bone tissue as well. This distinction is meaningful from a diagnostic point of view: hard tissue injuries are relatively easy to detect, while soft tissue injuries are typically not.

Injury mechanism categorization may be achieved by several ways: one of the most popular is based on the global movement of the head relative to the torso that is: compression, tension (or distraction), flexion, extension, rotation and coupled movement of the aforementioned ones (Cusick and Yoganandan, 2002; King, 2018a) (**Figure 28.**) However, only a few modes of mechanisms are relevant: compression, compression and flexion, compression and extension, and rotation (King, 2018a). It is also worth noting that this classification can be misleading with regards to recognizing the actual injury mechanism. Frequently, the motion of the head is different from the motion of the injured cervical segment. For instance, a flexion motion of the head may be simultaneously present with an extension motion of a spine segment. In addition to that, a local injury of a spine segment may occur before any global head motion is observable (Nightingale et al., 2015).

Main force vector	Coupled force component	Resulting injury
Axial	Compression	Jefferson fracture Burst fracture
Flexion	Hyper-	Ligamentous instability
	Compression	Wedge fracture Tear drop fracture
	Distraction	Bilateral facet dislocation
	Shear	Odontoid fracture Transverse ligament compromise
	Rotation	Unilateral facet dislocation
Extension	Hyper-	Ligamentous instability
	Compression	ALL compromise Vertebral arch fracture Vertebral body fracture
	Distraction	Spondylolisthesis of C2 Anterior C1 fracture Occipital-cervical dislocation Hangman's fracture
	Shear	Odontoid fracture Atlanto-axial dislocation

Table 1. Illustrative list of injuries based on the mechanistic categorization of injuries (Cusick and Yoganandan, 2002)

Compression can lead to a special kind of injury, which is called *Jefferson fracture* (Jefferson, 1919). This injury mechanism is recognizable by the fracture of the anterior and/or posterior arches of the atlas. Another commonly occurring type is burst fracture, which involves the disintegration of one of the vertebral bodies and piercing of the spinal cord by bony fragments (King, 2018a).

Compression-flexion occurs when an eccentric compressive force acts upon the head, leading to wedge fracture, burst fracture, or anterior dislocation of the cervical vertebrae. In severe cases, dislocation frequently leads to quadriplegia due to greatly injuring the spinal cord. A typical instance of this injury mechanism is the case when the rider is thrown over the vehicle during a motorcycle crash and the head impacts on road surface (King, 2018a).

Compression-extension cause injuries to the spinous processes. However, nowadays this type of injury mechanism occurs only when the occupant doesn't use the seat belt. In frontend

crashes, the unrestrained occupant slides forward and upward, which can cause the head to extend and impact on the windshield (King, 2018a).

Tension-extension loading is also a common one, resulting in the Hangman's fracture and disruption of anterior ligaments of the cervical spine. Tension-extension injury mechanism is suffered by, for instance, unbelted occupants whose heads hit the windshield while their torso move forward (Chen et al., 2011). A summary and other injury mechanism type are included in **Table 1**.

Since major injuries predominantly occur during approximately the first 10 ms and muscle activation is reported to be 60 ms, pre-injury state of muscle activation greatly affects the resulting mechanics of the damage but post-trauma muscle activation does not (Cusick and Yoganandan, 2002; Chancey et al., 2003).

3.4. CERVICAL SPINAL INJURIES

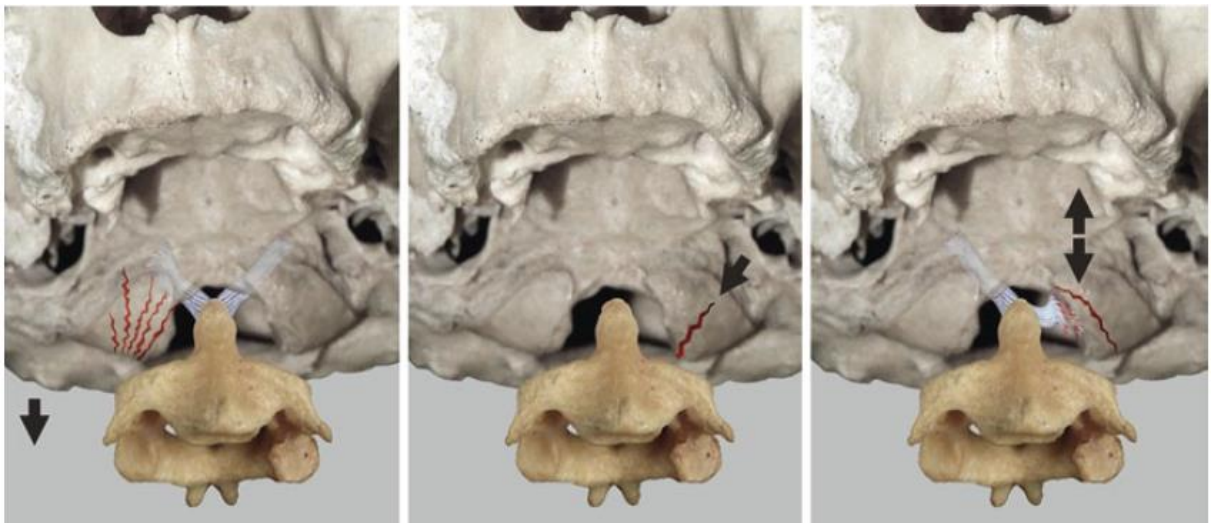

Figure 29. Occipital condyle fractures (Kandziora et al., 2010)

Burst fracture occurs due to severe compression forces, which result in complete destruction of the affected vertebral body. The fragments of the damaged bony parts often cause spinal cord injuries. The most common sites of this variety of injuries is at the level of C4, C5, and C6 (Nightingale et al., 2015).

Cervical spine dislocation, i.e., subluxation of the superior vertebral body relative to the adjacent, inferior vertebra, is often accompanied with disruption of the intervertebral discs and dislocation of the articular facets. If both facets are displaced, *bilateral facet dislocation* is the term that is used to describe the condition. Bilateral facet dislocations are also associated with fractures of the facets and of the lips of the vertebral bodies. Also, the frequent result of this type of injury includes spinal cord damage. However, when only one articular facet is displaced anterosuperiorly relative to the subjacent vertebra, *unilateral facet dislocation* occurs. The chance of spinal cord injury due to unilateral facet dislocation is relatively slight, although the injury remains asymptomatic, which prevent proper diagnosis and care (Nightingale et al., 2015).

One the most frequently mentioned lesion of the upper cervical spine is the *Jefferson fracture*, which is a four part fracture due to axial compressive forces (Nightingale et al., 2015) (**Figure 30.**)

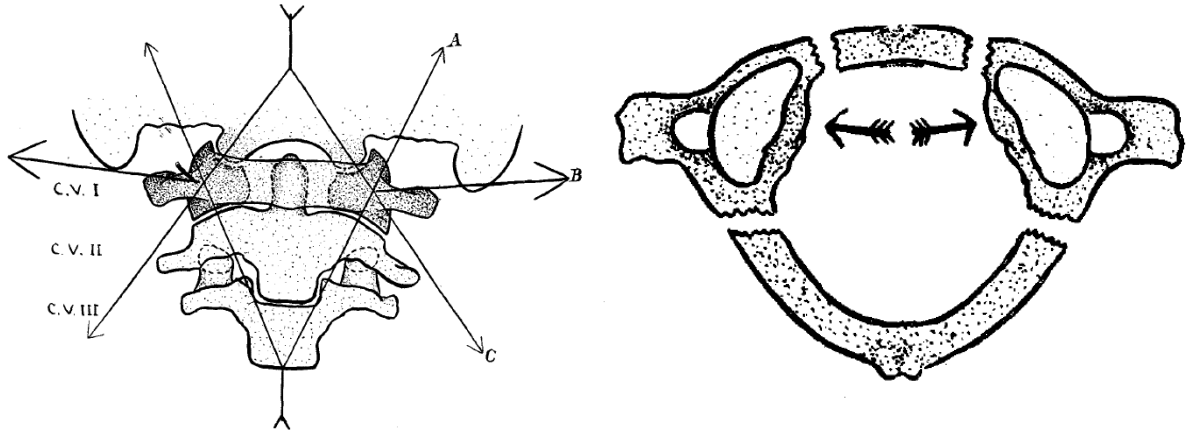

a) b)

Figure 30. a) Posterior view of the upper cervical spine: mechanism of Jefferson fracture b) Resulting view of Jefferson fracture (Jefferson, 1919)

Hangman's fracture refers to the disruption of the neural arch of the axis near its laminae (**Figure 31.**) As the name suggests, this lesion most commonly occurred due to judicial hanging. Nowadays, mostly high-speed vehicular crashes cause this type of fracture (Nightingale et al., 2015) when the occupant's chin hit the steering wheel, which directs the head to a severe extension state.

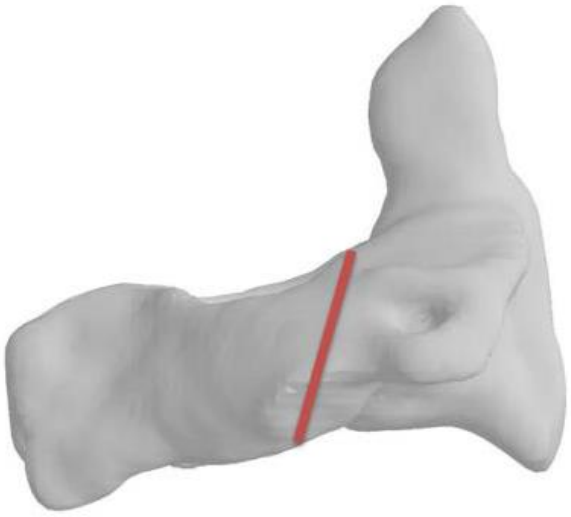

Figure 31. Hangman's fracture of axis (Nightingale et al., 2015)

Odontoid fractures involve lesions to the odontoid process of the axis (**Figure 32.**) The danger of this type of fractures lies in the fact that the strongest ligaments connecting the head to the spine attaches to the dens. Therefore odontoid fractures may easily lead to atlanto-axial dislocation, which, in turn, causes severe lesion of vital vascular and neurological structures

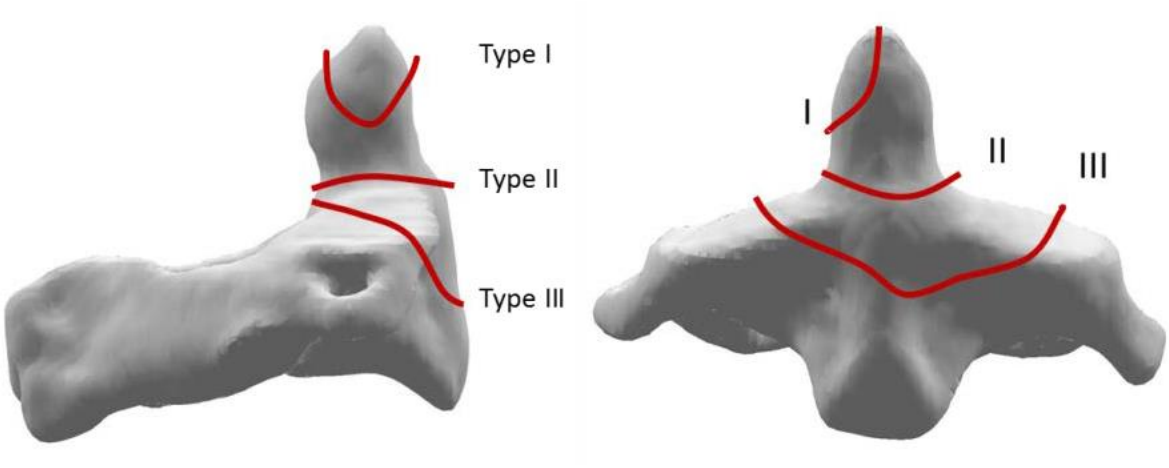

a) b)

Figure 32. Odontoid fracture of the axis (Nightingale et al., 2015)

Another notable injury type is the basilar skull fracture. Attention to this kind of generally fatal injury was drawn by high speed race car crashes. Since the main blood vessels of the head are torn apart during a basilar skull fracture and direct damage occurs to the brain, this type of injury has a high fatality rate (Nightingale et al., 2015).

3.5. LABORATORY TESTS

Experimental investigations are essential in exploring the behavior of the cervical spine under various conditions since these investigations provide validation data for numerical models. Validation of computational models is most commonly based on relatively easily measurable quantities of experiments, such as quasi-static or dynamic global head movement, range of motion of spinal segments due to applied, measured, loads.

The conducted experimental research data are numerous; however, there are only a few type of tests that are most commonly carried out. For instance, one can distinguish between *static* and *dynamic tests*. Another categorization might be the fact that whether the investigated specimen is alive or not. Based on this, there are *in vivo* and *in vitro* test, respectively. Also, in case of in vitro measurements, a further categorization can be made: *whole cadaver* or *segment tests* can be conducted. In addition, with regards of the applied load, *flexion*, *extension*, *lateral bending* and *axial tests* can be distinguished. Besides these types of experiments, there are also, *range of motion tests* and *tolerance tests*. A few illustrative example follows.

Chiefly, bending tests are conducted on human cadaver cervical spines. A typical setting includes the head and the whole cervical spine while the former is acted upon by pre-defined loads and the latter is fixed at the vicinity of the T1 vertebra (**Figure 33.**) A similar setting is used to measure extension or lateral flexion response of whole cervical spines.

Another study was conducted to measure cadaver cervical spine tensile tolerance properties (Dibb et al., 2009). The effect of boundary conditions was also investigated.

The rotation-bending moment relationship of the cervical spine is commonly determined (Goel et al., 1988). Some researchers investigated even the effects of aging thus degeneration of the spine (Wheeldon et al., 2006).

Another fairly typical dynamic experimental setting includes a sled upon which a chair is fixed (**Figure 34.**) The sliding board is started at the top of the sled device, which is stopped by a pneumatic cylinder at the bottom. When the deceleration is produced by the pneumatic cylinder, the subject is under a similar condition that is present at vehicular collisions thus the response of the neck can be investigated (Kumar et al., 2005, 2006).

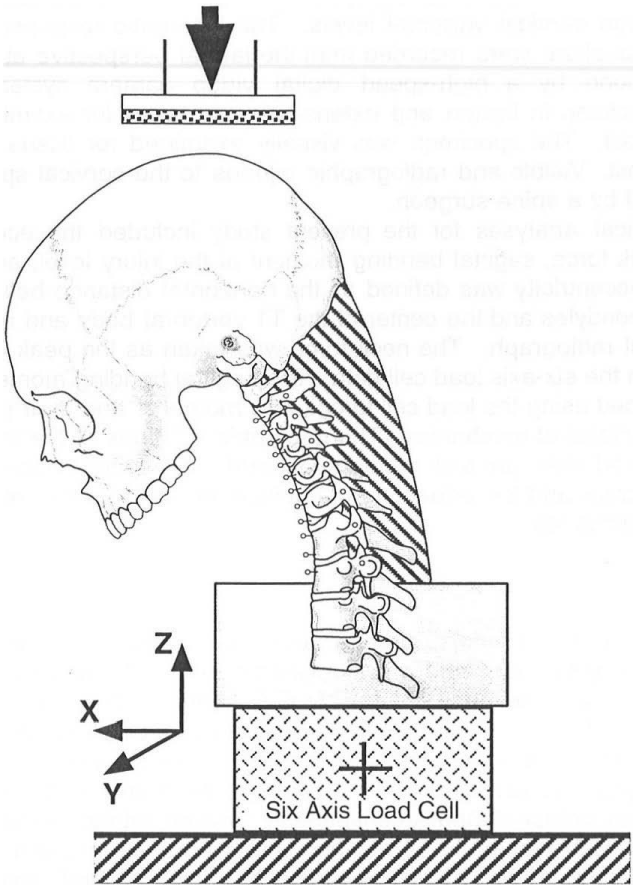

Figure 33. A typical experimental setting of a flexion bending test of human cadaver whole cervical spines (Pintar et al., 1998)

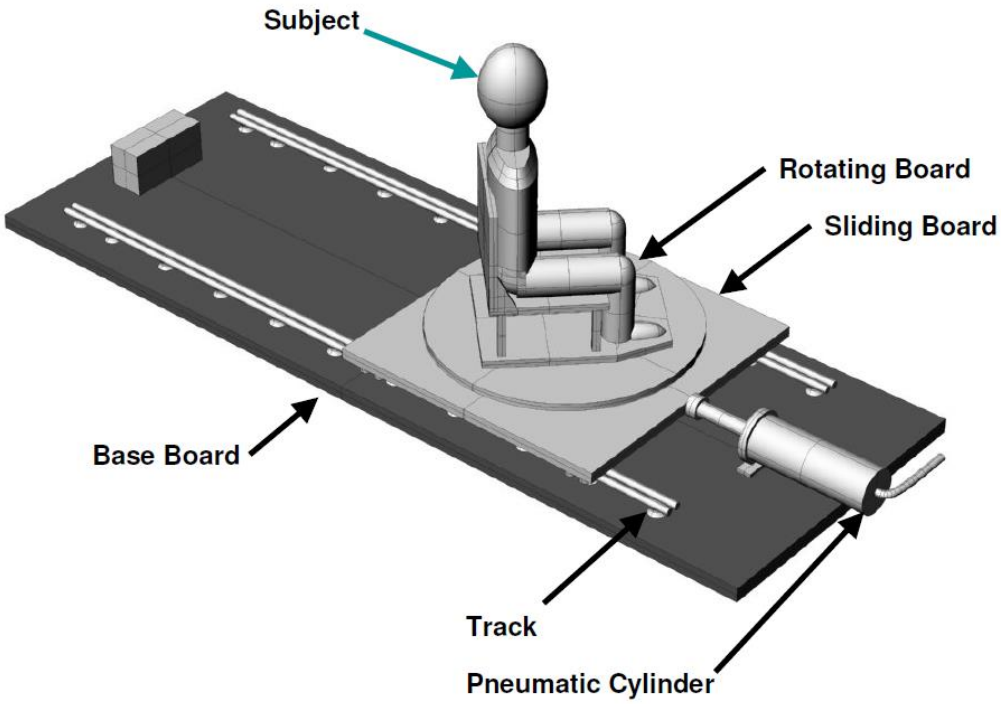

Figure 34. Sled device used in dynamic studies (Kumar et al., 2005)

3.6. FINITE ELEMENT MODELLING

There are several difficulties that hinders the process of enhancing our understanding of injury mechanisms. First, volunteers, during an experiment, cannot be subjected to loads that approach physiological tolerance levels, let alone exceeding them. When using cadavers, the main disadvantage is the unrealistic behavior of the muscles, which have great influence on the test results. Nowadays, several researchers turn to mathematical modeling, including finite element modeling, in order to handle these difficulties. The automotive industry adopted a mixed approach: crash tests' data is used in FEM simulations to investigate internal and local effects on the human body. Here, the biofidelity of the dummies is questionable since ligaments of the cervical spine are not modeled. However, the results can still be used for comparative purposes (Golinski and Gentle, 2001).

3.6.1. MAIN TENDENCIES OF MODELLING

Before taking a close look at the different modelling practices found in the literature, an important factor ought to be mentioned, which greatly affects the modelling approach, namely: whether the finite element analysis is planned to be *static* or *dynamic*. The characteristics of each is heavily affected by current computational limits.

Static models represent the cervical spine with higher complexity geometrically as well as constitutive model-wise (**Table 2.**). However, only segments of the spine are commonly analyzed. Mostly, the inferior surface of the lowermost modelled vertebra is fixed and moment loads are defined at the uppermost part of the model. In case of the majority of static cervical neck models, muscles are not included (Sokol et al., 2014).

Dynamic models, on the other hand, often incorporate the whole cervical spine and the head but the accuracy of constitutive and geometrical models are limited (**Table 3.**). Frequently, vertebral bodies are modelled as rigid bodies and soft tissues as linear springs. However, muscles are typically included in the model.

Author	Vertebra	Int. disc	Ligaments	Facet joints	Segment
Kumaresan et al., 2000	Segmented solid	Segmented solid: fibers, fluid	Nonlinear elastic bar	Nonlinear solid and membrane	C4-C6
Greaves et al., 2008	Linear solid	Linear link elements	Linear tension only link elements	Link elements	C4-C5
Wheeldon et al., 2008	Linear segmented solid	Nonlinear segmented, detailed solid	Nonlinear spring	-	C4-C7
Toosizadeh and Haghpanahi, 2011	Anisotropic linear solid cortical and cancellous bone	Hyperelastic solid NP, AFGS, nonlinear tension-only link AF	Nonlinear tension-only spring element	Contact elements	Occiput + C1-C7
Han et al., 2012	Linear solid and linear shell	Solid NP and solid AF and truss fibers	Tension only linearly elastic truss	Contact elements	Head + C1-C7
Bredbenner et al., 2014	Solid	NP and viscoelastic solid AF	Nonlinear spring element	Contact elements	C3-T1
Sokol et al., 2014	Segmented Solid	Segmented solid	-	-	C1-L5
Teixeira et al., 2015	Linear solid	Segmented linear solid	Linear tension-only spring elemnts	contact elements	C5-C6
Östh et al., 2016	Elasto-plastic shell and solid	Viscoelastic solid NP, hill foam solid AF and nonlinear orthotropic shell	Nonlinear shell	Linear solid	Head + C1-T1

Author	Vertebra	Int. disc	Ligaments	Facet joints	Segment
Zafarparandeh et al., 2016	Linear segmented solid	Incompressible fluid element NP and hyperelastic AF and tension-only fibers	Tension-only, linear truss elements	Contact elements	C2-C7
Subramani and Justin, 2016	Linear solid	Nonlinear segmented solid	Linear bar element	-	C4-C5
Wei et al., 2017, p. 7	Elasto plastic shell and solid	Hill foam AFGS fabric shell AF fibers and viscoelastic solid NP	Non-linear beam	linear solid cartilage endplate + linear solid articular cartilages	Head + C1-C7

Table 2. Summary of static FEM models

Author	Vertebra	Int. disc	Ligament	Muscle	Facet joints	Segment
Jost and Nurick, 2000	Elasto-plastic shell: cortical bone	Nonlinear elastic solid with spring- damper	Linear elastic shell with spring-damper	Linear elastic shell with spring-damper	Contact	head + C1-T1
Golinski and Gentle, 2001	Rigid shell	Blatz-Ko rubber solid	Nonlinear (FDC) shell with spring	Nonlinear spring	-	dummy + C1-T1
Choi et al., 2002	Rigid body	Nonlinear elastic joint element	Nonlinear elastic bar element	Bar element	-	head + C1-C7
Brolin et al., 2005	Linear visco-elastic shell and solid	Linear elastic membrane and solid	Nonlinear, tension-only spring and membrane	Nonlinear spring	frictionless contact, linear solid cartilage	head + C1-T1
Zhang et al., 2005	Segmented elasto-plastic shell and solid	Linear solid AF and linear solid NP	Nonlinear cable and brick elements	-	Surface contact elements	Head + C1-C7
Panzer, 2006	Solid and shell	AF: shell+solid	Nonlinear cable elements	Hill-type cable elements	Solid cartilage and pressure-volume airbag model for synovial fluid	head + C1-T1
Teo et al., 2007	Zhang et al., 2005	Zhang et al., 2005	Zhang et al., 2005	-	Zhang et al., 2005	Head + C1-C7
Brolin et al., 2008	Rigid or linear viscoelastic shell cortical and solid cancellous	Linear elastic, anisotropic membrane AF linear viscoelastic solid AFGS linear elastic NP	Linear elastic membrane and nonlinear cable	Hill-type, or bilinear cable	Linear elastic solid and sliding-only contact	Head + C1-C7
DeWit and Cronin, 2010	see Panzer, 2006	adopted from Panzer, 2006	Nonlinear tension-only beam elements	-	see Panzer, 2006	C4-C5
Panzer et al., 2011	Rigid body	Hyperelastic solid GS Nonlinear elastic membrane AF Linear viscoelastic solid NP	Strain rate dependent beam	Hill-type beam	Linear viscoelastic solid	Head + C1-T1
Zhang et al., 2011	Elasto-plastic solid	Linear solid AF and viscoelastic solid NP	Linear solid and tension only cable	Nonlinear Hughes-Liu beam elements	-	Head + C1-T1

Author	Vertebra	Int. disc	Ligament	Muscle	Facet joints	Segment
Jost and Nurick, 2000	Elasto-plastic shell: cortical bone	Nonlinear elastic solid with spring- damper	Linear elastic shell with spring-damper	Linear elastic shell with spring-damper	Contact	head + C1-T1
Golinski and Gentle, 2001	Rigid shell	Blatz-Ko rubber solid	Nonlinear (FDC) shell with spring	Nonlinear spring	-	dummy + C1-T1
Fice et al., 2011	Solid	Solid AF, solid NP and shell fibers	nonlinear and rate dependent Truss elements	Hill-type solid and beam elements	Solid cartilage	Head + C1-T1
Dibb et al., 2013	Rigid body	Nonlinear viscoelastic beam	-	Sliding contact cable	-	head + C1-T1
Meyer et al., 2013	Rigid body	Linear solid elements	Nonlinear springs	Nonlinear BC	-	head + C1-T1
Wang et al., 2018	Linear shell and ortothropic linear solid	Hill foam solid AF ground substance rebar layer fibers viscoelastic solid NF	Nonlinear spring	-	-	Head + C1-C7

Table 3. Summary of dynamic FEM models

3.6.2. EXAMPLES OF MODELLING DETAILS AND DIFFICULTIES

In the next few paragraphs, a few interesting example of modelling issues are described in an unsystematic order. The aim of this absolutely not exhaustive list is to prepare for the same difficulties when developing the cervical neck model.

Modelling the facet joints comes with a difficulty: synovial fluid cannot be simply modelled with finite elements because those elements distorts greatly even for physiological loads, which result in numerical problems. However, omitting the synovial fluid creates an unrealistic spine behavior. Therefore hydrostatic pressure is set to act on the proper surfaces of the facets to model synovial fluid (Panzer, 2006).

When validating the cervical spine model, a common approach is that the material model characteristics are calibrated so that the numerical model mimic some experimental response. Even though global kinematics can reliably be reconstructed, the problem with calibrating is that the main point of it is to compensate for some modelling deficiencies. Thus tissue-level response is likely to be far from biofidelic. To overcome this discrepancy, a model developing ought to take place at tissue level as far as the geometry and material properties are concerned (Panzer et al., 2011).

In order to account for realistic change in direction of line of action of muscles, intermediate points ought to be inserted, which then constrained to the vertebra, over which it spans (Dibb et al., 2007; Panzer, 2006). This consideration is emphasized by many (Brolin et al., 2005; van der Horst et al., 1997).

Obviously, the head-neck complex is unstable without the forces that arise due to muscle activation. However, finding the realistic muscle forces required to the equilibrium of the cervical spine under only gravitational load is a separate and problematic issue. Also, several authors noted that gravitational effects are negligible in comparison with live loads therefore the former effects are commonly not taken into consideration (Dibb et al., 2013). However, some authors made the assumption that all muscles are fully tensed during simulation thus making their model more biofidelic (Dibb et al., 2013). Other authors used a parallel element approach to simultaneously model muscle active and passive properties (de Bruijn et al., 2016).

The materials of the human body are mainly visco-elastic and strain rate sensitive but can be relatively realistically modeled with elasto-plastic material model, which also greatly

reduces the computational time (Jost and Nurick, 2000).

Also, one important aspect of modeling the cervical spine is considering anatomical variation and asymmetry. Studies show that, despite of the massive efforts to create symmetric load conditions, asymmetry in fracture mechanism is observed (Nightingale et al., 2015).

To simplify the analysis, (Jost and Nurick, 2000) defined only the cortical bone tissue, with greater mass density to produce a similar inertial behavior of the vertebra.

4. DEVELOPMENT OF THE FINITE ELEMENT MODEL

4.1. GEOMETRY

In order to produce a biofidelic response, sufficient amount of details ought to be included in the geometrical model. Fortunately, there has been a huge effort to build a full human body geometry model. The improved work of Mitsuhashi et al., 2009 was used to build the geometrical model of the bones (Hamer, 2018).

The general overview of the definition of the geometrical model is as follows. The relevant parts of the skeleton were loaded in Spaceclaim (*SpaceClaim*, 2018) in order to additionally define ligaments and muscles as line bodies in between bones. Then, when all the geometrical model of the whole head-neck complex were loaded into Ansys Mechanical (*ANSYS Mechanical*, 2018).

More precisely, the following bony parts are modelled: **skull without mandible**, **atlas**, **axis** and **C3 vertebra**. As far as the soft tissues are concerned, the **intervertebral disc between the axis and C3 vertebra**, and **ALL**, **PLL**, **LF**, **ISL**, **CL**, **AAAL**, **PAAL**, **TL**, **AAOM**, **PAOM** and **TM** ligamentous structures, and **MIS**, **MIT**, **MR**, **MOCS** and **MRCPMi** of the muscles were included (**Table 4.**) Besides, fictional cartilage was also built in in order to establish a simple connection between the skull and the atlas. Another fact worth paying attention to is that the mandible was neglected in order to simplify the meshing process and also reduce the numbers of finite elements.

Soft tissue	Cross-sectional Area/PCSA [mm^2]	Author
ALL	11,1 (1,93)	(Yoganandan et al., 2000)
PLL	11,3 (1,99)	
CL	42,2 (6,39)	
LF	46,0 (5,78)	
ISL	13,0 (3,27)	
TM	33,02 (5,46)	(Mattucci et al., 2013)
TL	18,89 (3,05)	
AAOM	87,03 (28,38)	
PAOM	48,84 (10,84)	
AAAL	50,34 (-)	
PAAL	21,55 (-)	
MIS	16,18 (-)	(Borst et al., 2011)
MR	24,27 (-)	
MIT	17,64 (-)	
MRCPMi	90,3 (-)	
MOCS	92,2 (-)	

Table 4. Used geometrical data of soft tissues

4.2. MATERIAL MODELS

As a first step, only homogenous, isotropic, linearly elastic material models are applied

(**Table 5.**) Since most of the materials that are constituent of the cervical spine are relatively complex, the material model itself and the assigned parameters (Young's modulus and Poisson's ratio) are no other than a first approximation.

For the bone tissue, finding the proper linearly elastic material parameters was quite easy as the bone bears the greatest resemblance to solid materials. Cancellous bone tissue was neglected and human cortical bone tissue material parameters were assigned to the bony parts of the model. However, human soft tissues behave drastically differently than solid bodies in general thus their linear material parameters are only suggestions or based on intuition. In addition, proper mass density data was not found for ligaments and intervertebral discs as a whole therefore the same value was assigned to them as it was to articular cartilage. This choice may be justified by the fact that the aforementioned three soft tissue have similar inner structure (Korhonen and Saarakkala, 2011).

As it was discussed, intervertebral discs interior structure is quite complex. However, while building the model, a homogenous and isotropic material behavior was presupposed therefore the nucleus pulposus and the annulus fibrosus was neglected as separate structures. Their combined overall behavior is represented by a linearly elastic, homogenous solid body.

Ligaments and muscles are incorporated into the model so that they resist only tension therefore their behavior follows the linearly elastic model in tension and produce no force in compression.

Most of the ligaments were modelled by more line bodies with circular cross sections in a way that the sum of the cross-sectional area of the constituent line bodies are equal to the ligaments' cross-sectional area reported in the literature (**Figure 35.**) However, each muscle is represented by one line body.

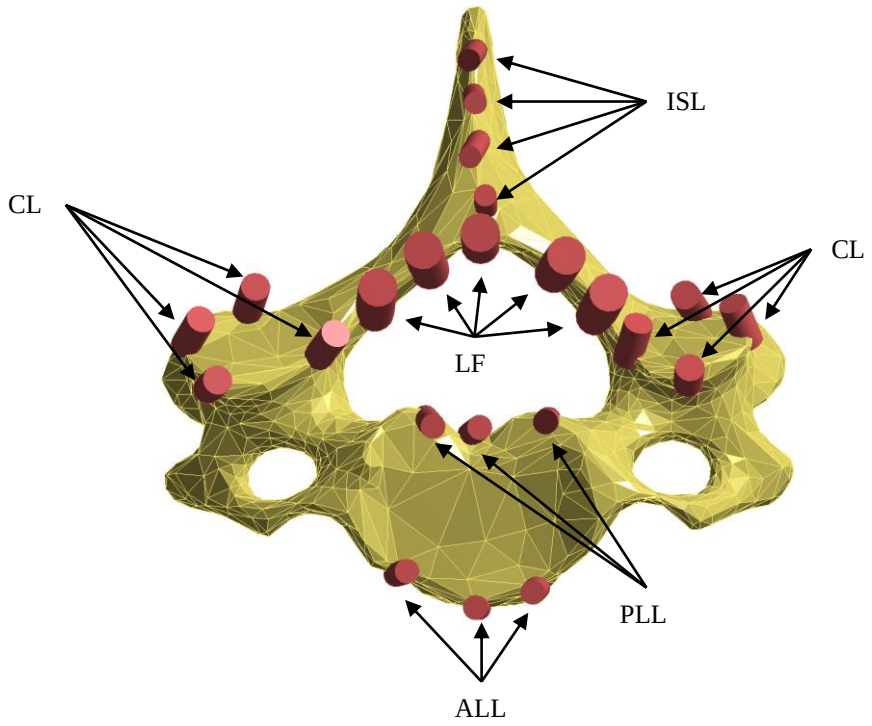

Figure 35. Superior view of C3 with ligaments connecting C3 to C2

Since the human head is not fully taken into consideration with all of its hard and soft tissues, a nominal mass density is assigned to the skull. Thus the inertial properties of the modelled skull are similar to the whole human head. Based on the data of average human head mass (m_{head} = 4729 g) reported by Clauser et al., 1969 and measuring the volume of the

geometrical model of the skull (V_{skull} = 497,3 cm^3), the nominal mass density of the skull (ρ_{skull}) was calculated as follows:

$$\rho_{skull} = \frac{m_{head}}{V_{skull}} \quad (1)$$

Besides, the mass density of the vertebrae were also calibrated due to the presumption of the vertebrae having homogenous material characteristics. Furthermore, cortical bone tissue mass density is almost twice as much as cancellous bone tissue, which also necessitates homogenization of the density. Based on the same riport (Clauser et al., 1969), density values of 1,80 g/cm^3 and 1,105 g/cm^3 were extracted for cortical and cancellous bone, respectively. A thickness of 1 mm was assumed for the cortical bone (Pan et al., 2019). With the help of the geometrical models, the volumes of the cortical bone tissue and the whole vertebra can be easily measured. The axis vertebra was used as a basis of the calculations.

$$\rho_{vert} = \frac{V_{cort} \cdot \rho_{cort} + (V_{vert} - V_{cort}) \cdot \rho_{canc}}{V_{vert}} \quad (2)$$

In (2), the variables have the following meaning:

- ρ_{vert} – mass density of the vertebrae
- V_{vert} – volume of the axis vertebra, V_{vert} = 12,892 cm^3
- ρ_{cort} – mass density of the cortical bone
- V_{cort} – volume of the cortical bone tissue in axis vertebrae, V_{cort} = 5,118 cm^3
- ρ_{canc} – mass density of cancellous bone

Tissue/Anatomical part	Mass density [g/cm^3]	Young's modulus [MPa]	Poisson's ratio [-]
Vertebrae	1,381	18000 (Pal, 2014)	0,4 (Korhonen and Saarakkala, 2011)
Skull	9,509	18000 (Pal, 2014)	0,4 (Korhonen and Saarakkala, 2011)
Ligaments	1,1	100 (Korhonen and Saarakkala, 2011)	0,4 (Korhonen and Saarakkala, 2011)
Intervertebral disc	1,1	100 (Meyer et al., 2004)	0,3 (Meyer et al., 2004)
Articular cartilages	1,1 (Pal, 2014)	10 (Pal, 2014)	0,4 (Korhonen and Saarakkala, 2011)
Muscles	1,0576 (Klein Breteler et al., 1999)	100	0,4 (Korhonen and Saarakkala, 2011)

Table 5. Applied material properties of the FE model

4.3. FINITE ELEMENT MESH

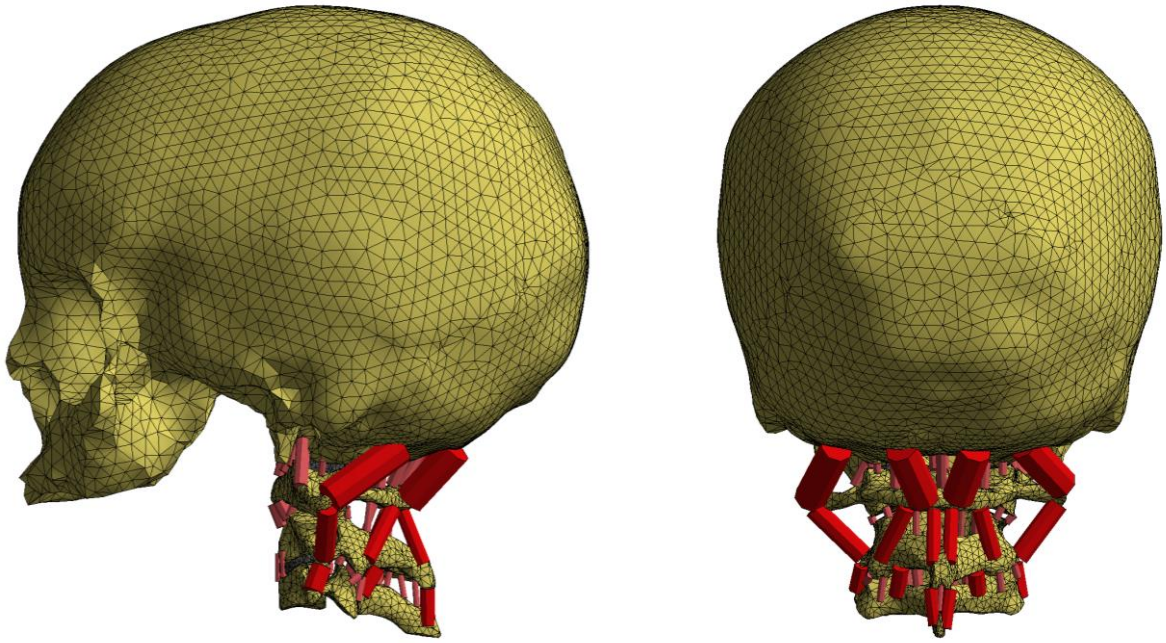

a) b)

Figure 36. a) Lateral view of finite element model b) Posterior view of the finite element model

Finite element mesh consists of quadratic tetrahedron elements (element type: SOLID187) and truss elements (element type: LINK180) resisting only axial forces (**Figure 36.** and **Figure 37.**) Logically, minimum element size is proportional to the volume and complexity of the body. For the skull, and the vertebrae and intervertebral disc, the minimum element size is set to 3 mm, respectively. In articular cartilage between the occiput and the atlas, the defined minimum element size is 1,5 mm. However, a different logic was applied to the line bodies in the model: each line body was meshed with only one LINK180 element.

a) b)

Figure 37. a) Lateral view of the neck b) Posterior view of the neck

Since LINK180 element has the capability of behaving like a truss (resisting tension as

well as compression) or being tension-only or being compression-only, it provided great flexibility in usage. All line bodies, representing ligaments and muscles, were set to be **tension-only**. However, in a later stage of the research, accounting for the active and passive behavior of the muscles will be one of the main tasks.

The geometric model, which provided the base for the mesh, is composed of several individual parts, which have no connections. This means that a key question of developing the finite element model is to establish proper connections between these separate parts. Between meshed bodies with 3D elements, contact elements were used to create a bonded connection meaning that these meshed bodies can neither slide relative to each other nor separate from one another. In case of joining line elements to 3D elements, line element nodes were connected to the nodes of tetrahedrons by several, automatically created beam elements. This connection lets the LINK180 elements to rotate but distributes the axial forces that are transmitted from these LINK180 elements.

4.4. APPLIED LOADS AND BOUNDARY CONDITIONS

Three types of loads were defined: gravitational load, a static and a dynamic load, each of which are distributed loads. In conjunction with all three loads, there's a fixed support distributed on the inferior surface of C3 (**Figure 38.**)

Three analysis were made: a **static**, a **modal** and a **dynamic**. **Static** analysis consists of **two subsequently applied load cases**. **First, only the gravitational** load was applied (Load Case 1) then, after finding equilibrium, a **static distributed force**, its resultant being 10 N, was applied while maintaining the gravitational load (Load case 2). Static distributed force points to the anterior direction (**Figure 38.**)

As far as the **modal analysis** is concerned, its sole purpose was to help defining a sufficiently small time step value and a sufficiently large duration for the dynamic analysis. The numerical results of modal analysis are not presented in the study. The effect of the first three mode was taken into account in the dynamic analysis by using the frequency of the third mode of the model:

$$\Delta t = \frac{1}{20 \cdot f_3} = \frac{1}{20 \cdot 16{,}963\ Hz} \approx 0{,}003\ s \tag{3}$$

where

- f_3 is the frequency of third mode,
- Δt is the applied maximum time step in the dynamic analysis.

Also, the frequency of the first mode was used to determine the length of the duration during which the response of the model was followed. This value was calibrated so that approximately 2,5 times period of the cyclic response would be captured by the analysis.

$$T = 2{,}5 \cdot \frac{1}{f_1} = 2{,}5 \cdot \frac{1}{10{,}439\ Hz} \approx 0{,}24\ s \tag{4}$$

where

- f_1 is the frequency belonging to the first mode,
- T is the duration of the followed response.

The **dynamic analysis** consists of no gravitational load and the same surface load as in the case of the static analysis but with a peak magnitude of 100 N (Load Case 3) (**Figure 39.**)

The dimensions of the results are indicated in the caption text of the figures. Also, the time instant of the presented results are found in the caption text.

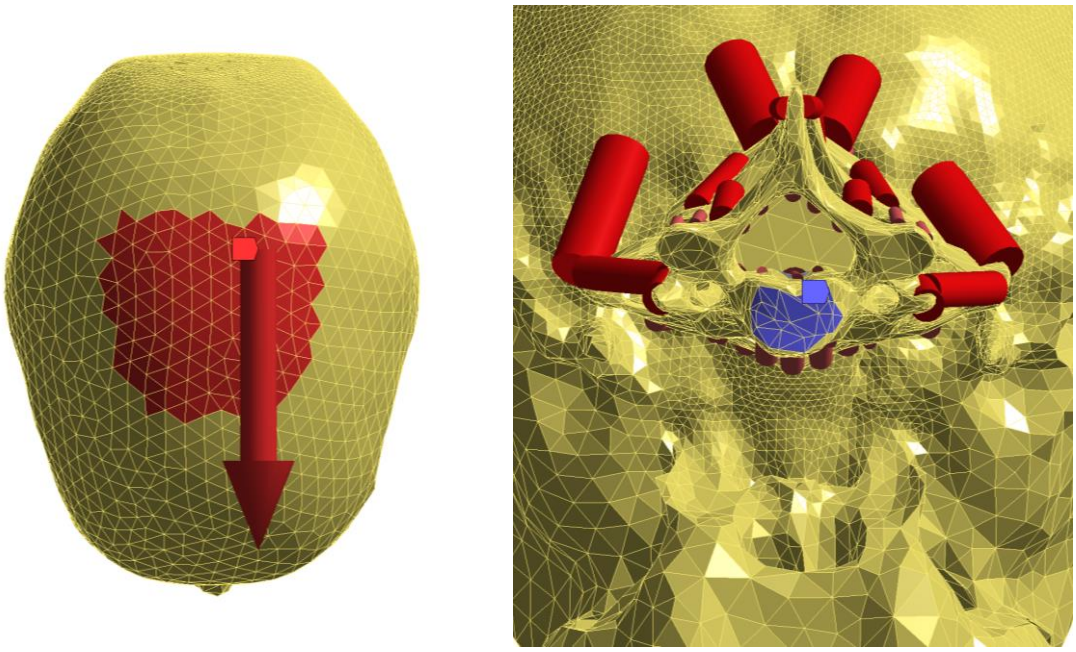

a) b)

Figure 38. a) Superior view of the cranium: surface over which the distributed loads are applied b) Inferior view of the model: surface over which the fixed support are set

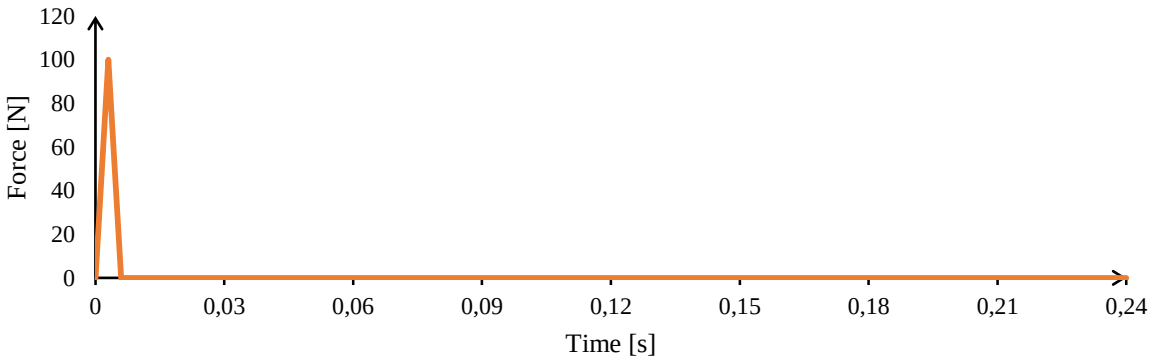

Figure 39. Dynamic force magnitude vs. time diagram

5. NUMERICAL RESULTS

5.1. LOAD CASE 1

Reviewing the results of the first load case, a slight flexion motion of the head can be seen on **Figure 40.** This phenomena may be justified by that fact that the gravitational center of the skull falls anteriorly relative to the spinal column.

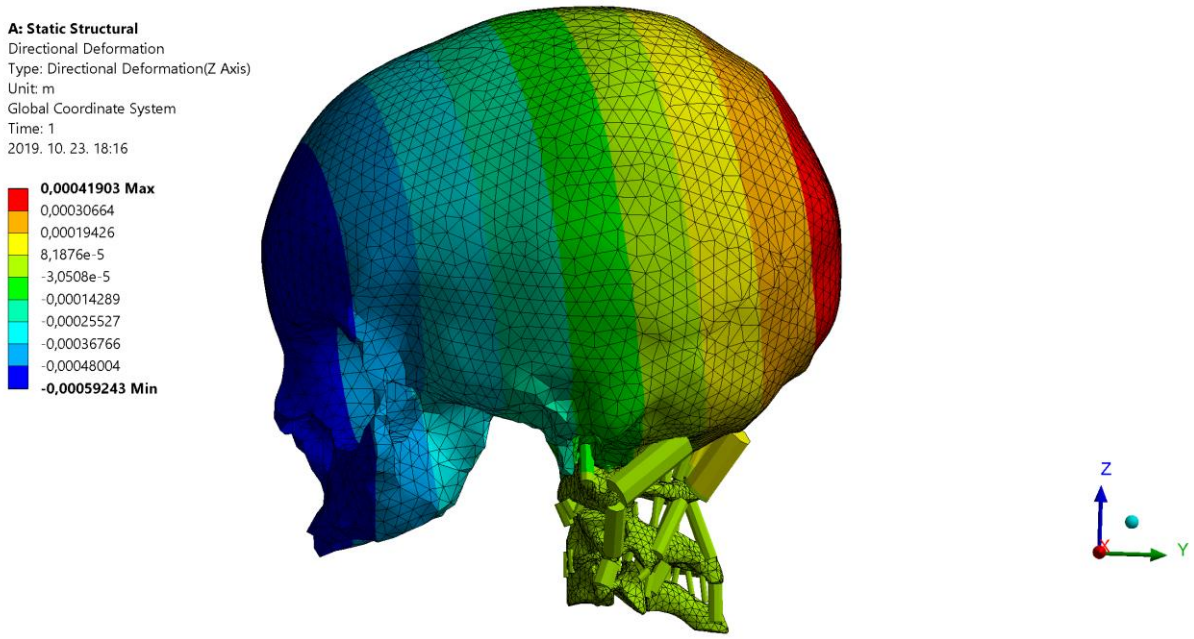

Figure 40. Lateral view: Z-directional displacement [m] due to gravitational load

Peak von Mises stresses arise in the posterior arch of the atlas near the lateral masses and the pedicles of C3 (**Figure 41.**) It seems, the posterior arch of C1 behaves almost as a cantilever: it is fixed at the lateral masses and is subjected to bending by the connecting soft tissues thus maximum stresses are produced at the lateral masses. A similar phenomena can be observed in the case of C3. Strangely, C2 vertebra remains unloaded compared to C1 or C3.

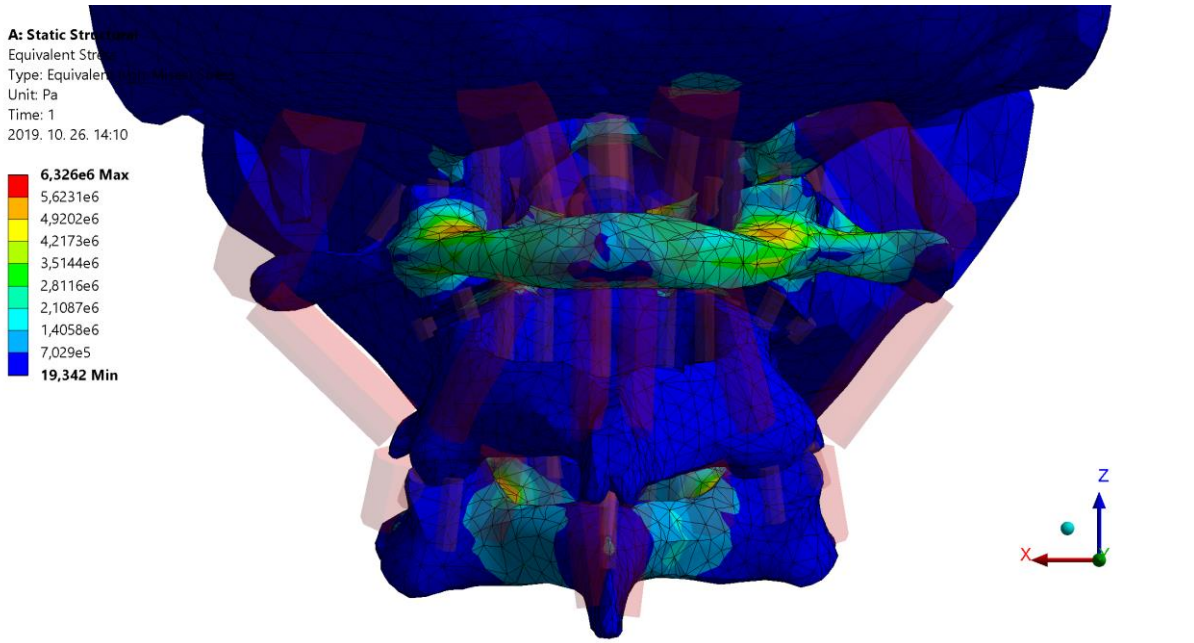

Figure 41. Posterior view: von Mises stresses [Pa] due to gravitational load

On **Figure 42.**, one can notice that the largest axial forces arise in muscles with the greatest cross-sectional area. Another observance is that the distribution of the axial forces are far from symmetric despite the fact that the model as a whole and the loads are approximately symmetric. Consequently, the resulting motion of the skull is also asymmetric.

Due to the asymmetric position of one pair of large muscles, the left MOCS becomes compressed thus exerts no resisting force. On the other hand, the MOCS on the right is under

tension therefore produces force. This two muscle may likely be the main contributors of the asymmetric motion of the whole system.

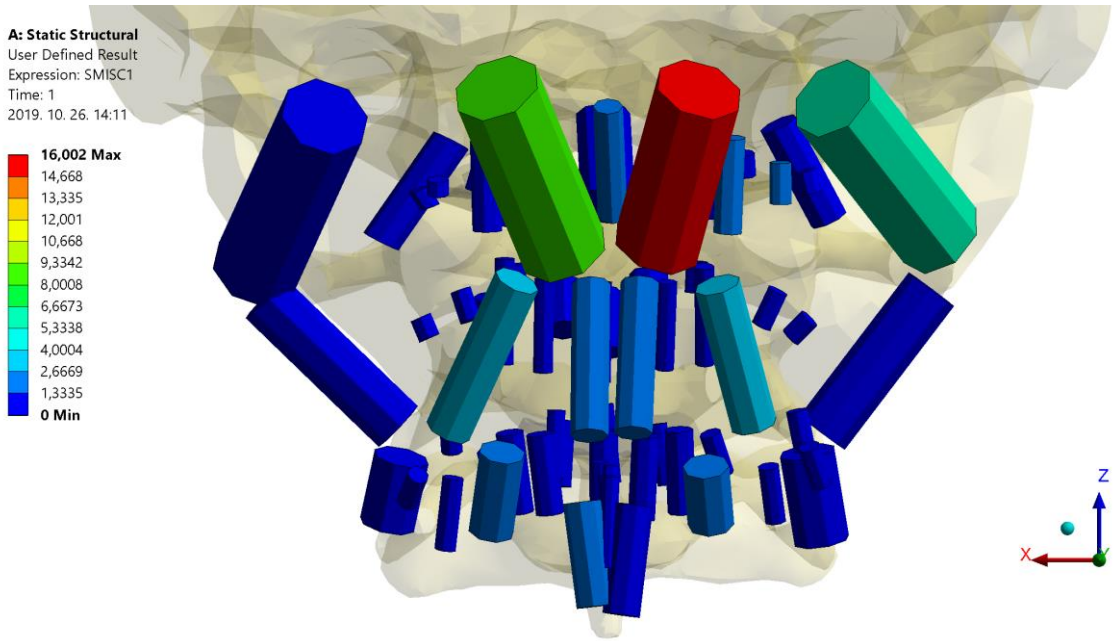

Figure 42. Posterior view: axial forces [N] of LINK180 elements of muscles and ligaments

5.2. LOAD CASE 2

A similar displacement field arises due to the applied force acting to the anterior direction (**Figure 43.**) The magnitude of the displacements are greater, as expected. The neck is clearly flexed to a small degree.

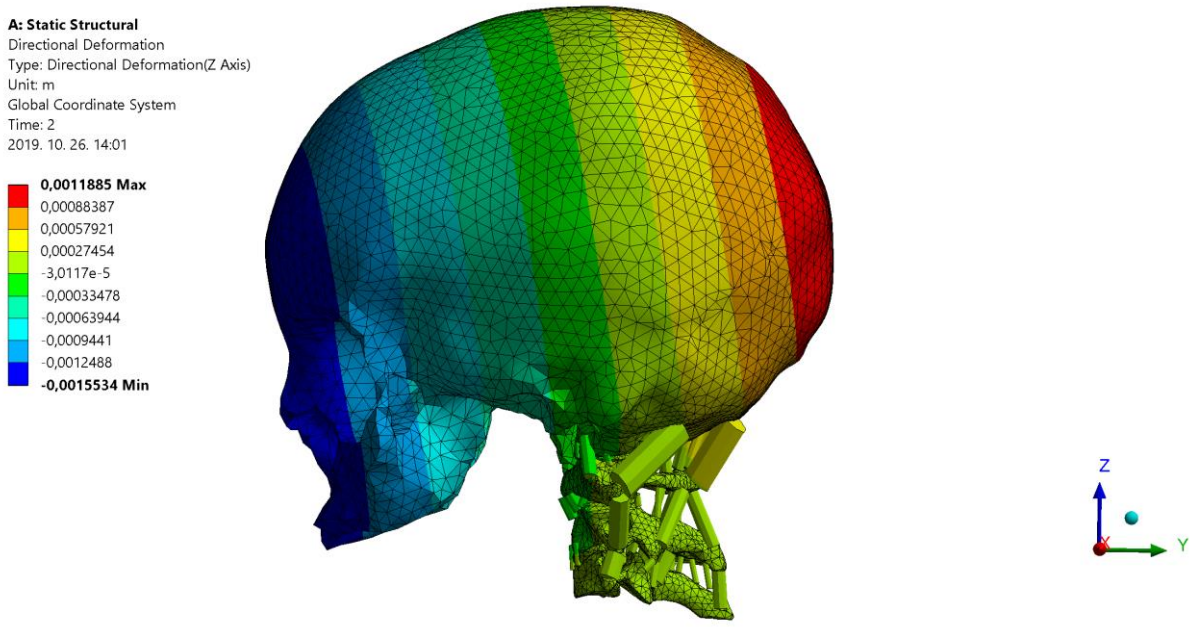

Figure 43. Lateral view: Z-directional displacement [m]

Stresses are now concentrated at the pedicles of C3 (**Figure 44.**) This may due to the definition of the supports. The vertebral body of C3 remains stationary while the posterior elements of C3 are pulled upwards by the connecting soft tissues thus peak stresses arise at the vicinity of the pedicles (**Figure 45.**) If elastic supports had been set, this stress concentration

may not have occurred during the analysis.

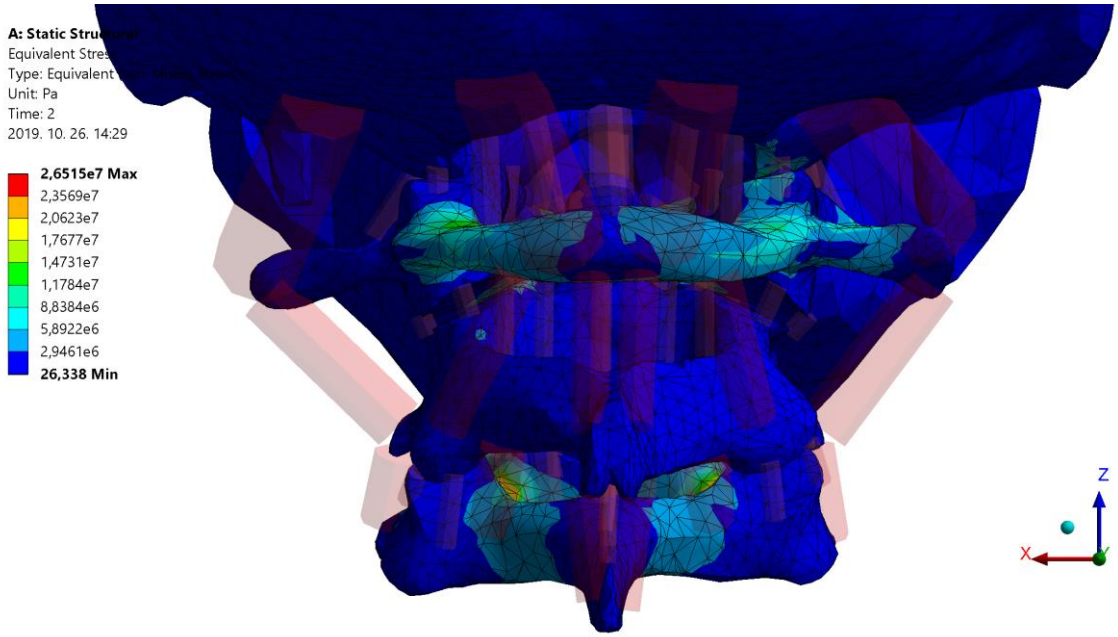

Figure 44. Posterior view: von Mises stresses [Pa]

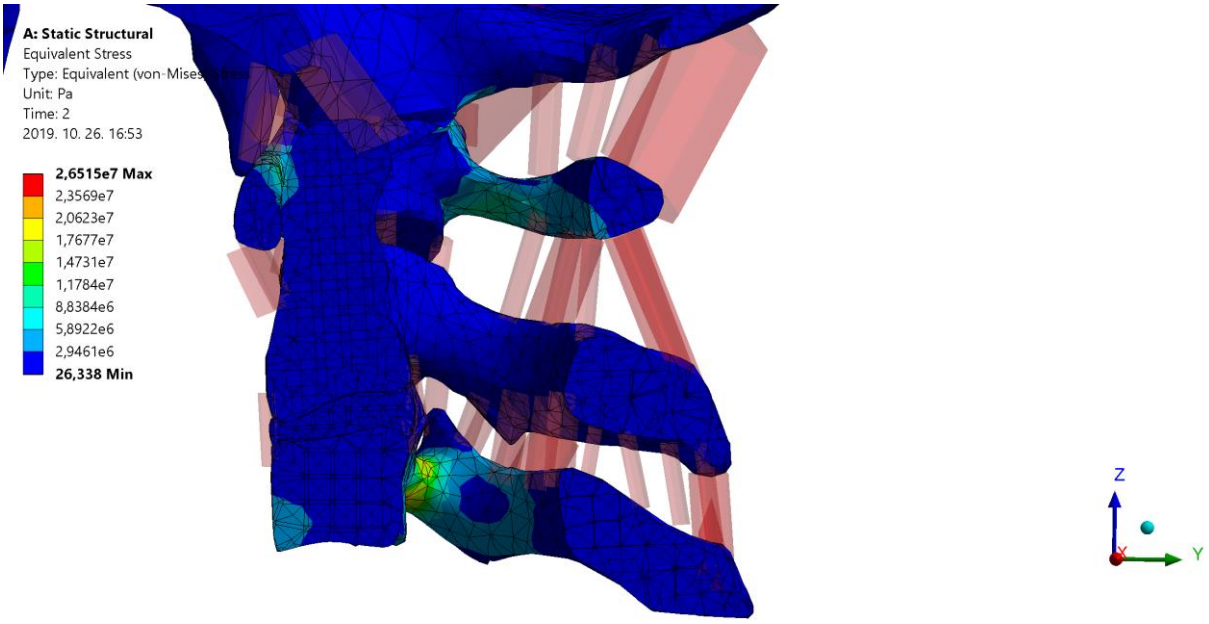

Figure 45. Cross section through the median sagittal plane: von Mises stresses [Pa]

Once again, a similar phenomenon occurred in case of the soft tissues (**Figure 46.**) The muscles with the largest cross sectional area exerts tensile force with uneven magnitudes leading to asymmetric motion of the skull.

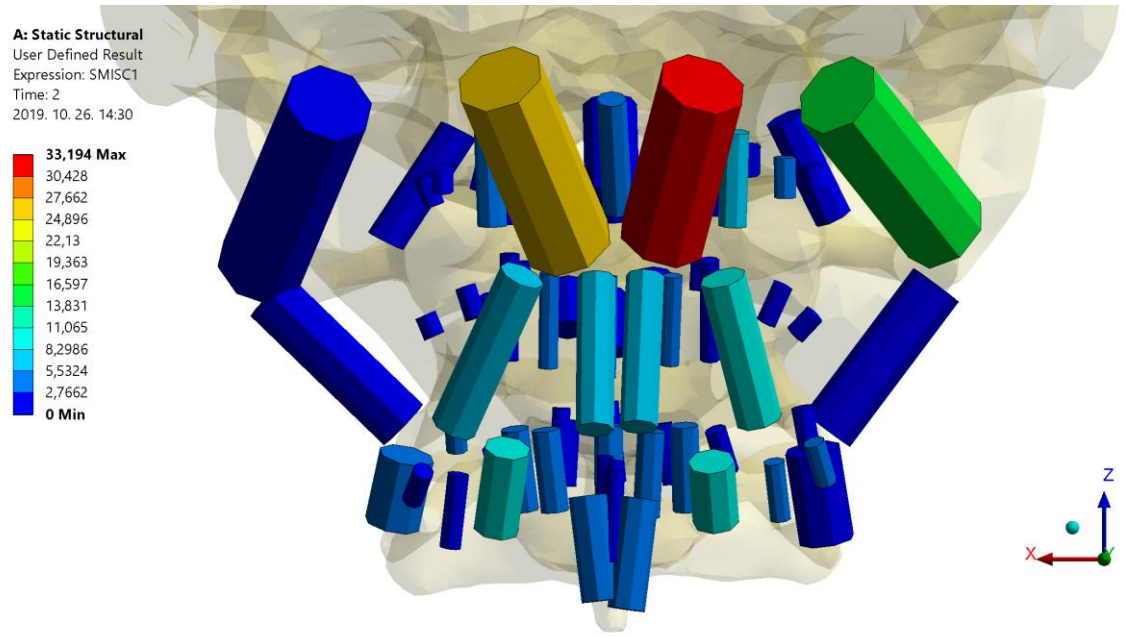

Figure 46. Posterior view: axial forces [N] of LINK180 elements of muscles and ligaments

5.3. LOAD CASE 3

Since the resulting displacement filed of the model is quite small, presenting the motion of the head by diagrams showing the displacement component vs. time is much more beneficial (**Figure 47.** and **Figure 48.**) Now we can see clearly the asymmetric motion of the skull: the X-directional displacements are in the same scale as the displacements' in the sagittal plane. Besides, the graph suggests that hardly any flexion motion was produced due to the applied distributed force since all component of the displacement of the skull's center of gravity takes on negative values to a very low extent.

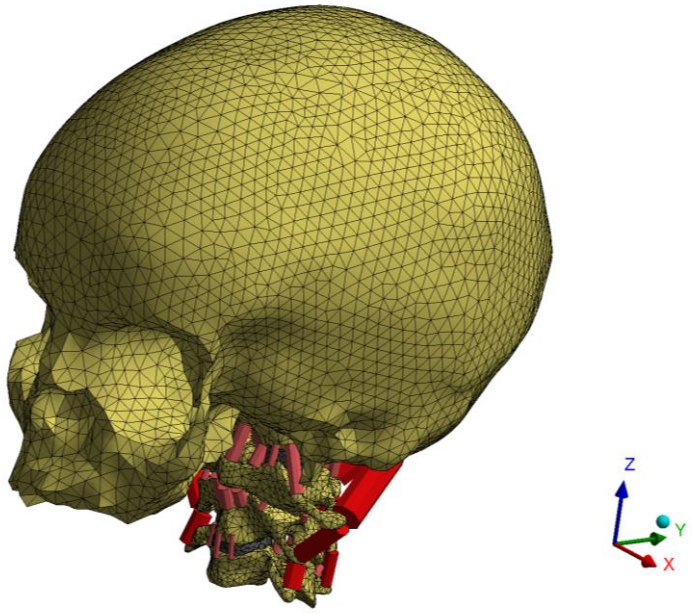

Figure 47. Finite element model with the coordinate axes

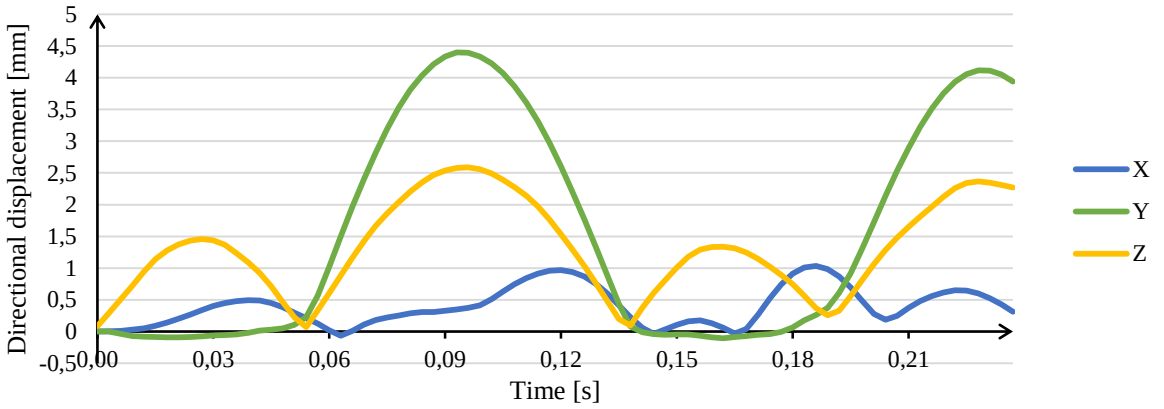

Figure 48. Directional displacement of the skull's center of gravity

As for the internal stresses and forces, a similar trend can be observed as it was in the case of static analysis results. In flexion, posterior arch of C1 and pedicles of C3 developed great peak stresses as the connecting soft tissues exerted tensile forces on them (**Figure 49.**) The axis still remained unloaded compared to other bony segments.

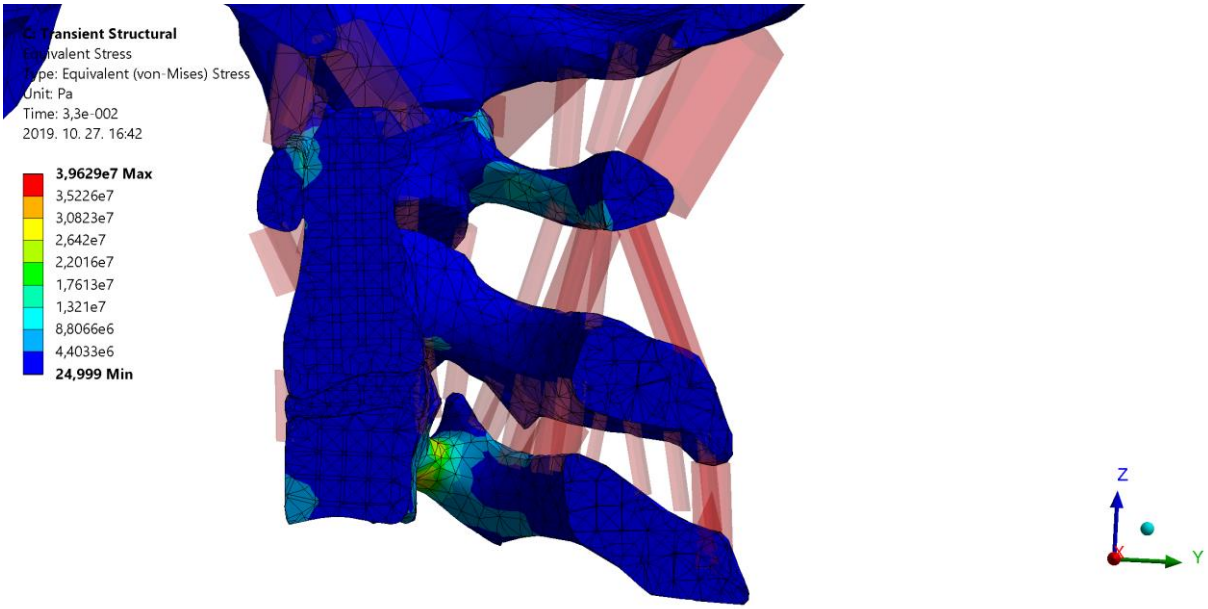

Figure 49. Cross section through the median sagittal plane: von Mises stresses [Pa] at time 0,033 s

In extension, peak stresses developed in the anterior arch of C1 and in the dens (**Figure 50.** and **Figure 51.**) This result may imply that the connection between C1 anterior arch and C2 odontoid process is poorly constructed.

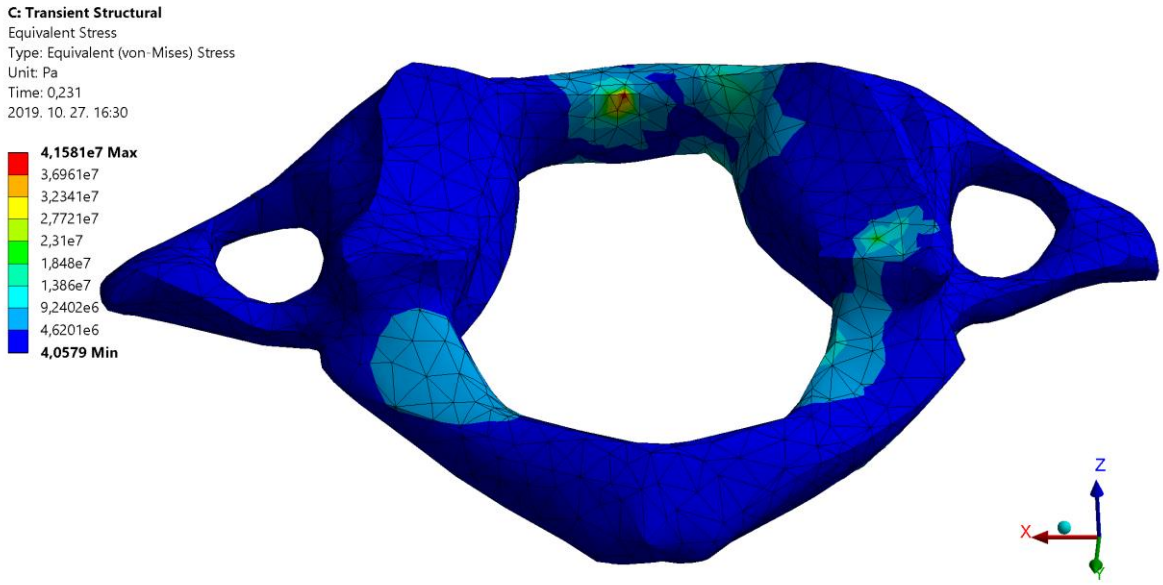

Figure 50. Superior-posterior view of C1: von Mises stresses [Pa] at time 0,231 s

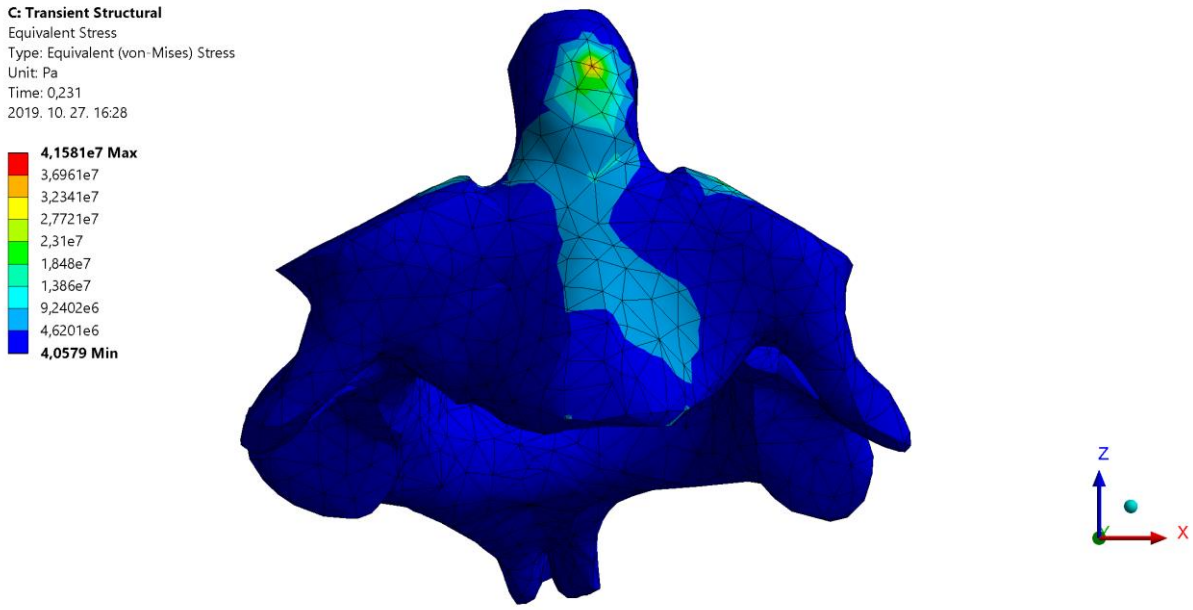

Figure 51. Anterior view of C2: von Mises stresses [Pa] at time 0,231 s

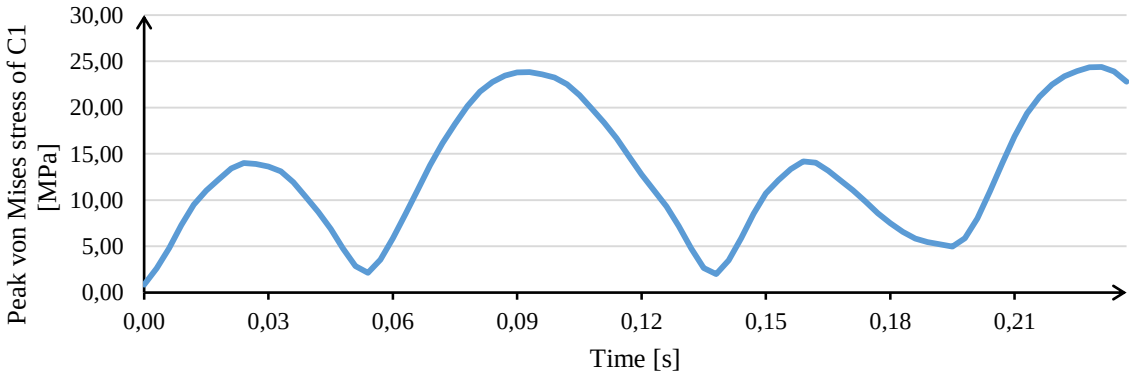

Figure 52. Peak von Mises stress [MPa] of C1 vs time diagram

Regarding soft tissues, their cable-like behavior can be clearly seen (**Figure 54.**, **Figure 54.**, **Figure 55.**, **Figure 56.**) In flexion, the posterior ligaments and muscles are in tension while in extension, the anterior soft tissues exert tensile forces. Especially, the maximum axial force is exerted by AAOM when the neck is in extension. However, PLL produces hardly any resistance during this flexion-extension motion.

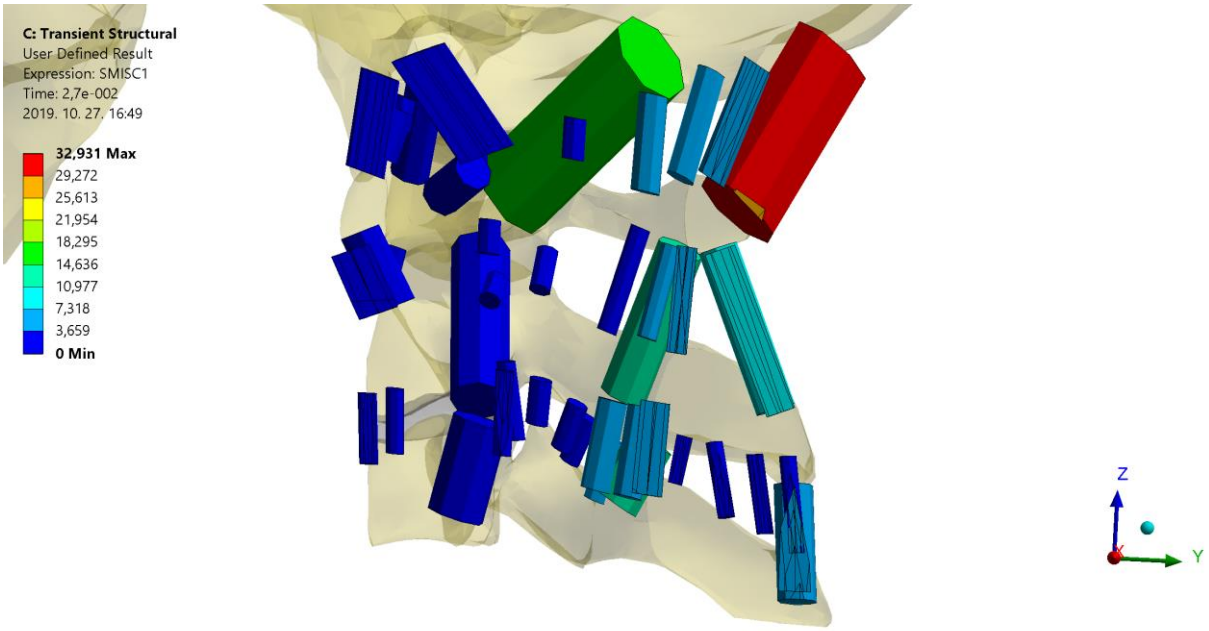

Figure 53. Cross section through the median sagittal plane: axial forces [N] of LINK180 elements of muscles and ligaments at time 0,0027 s

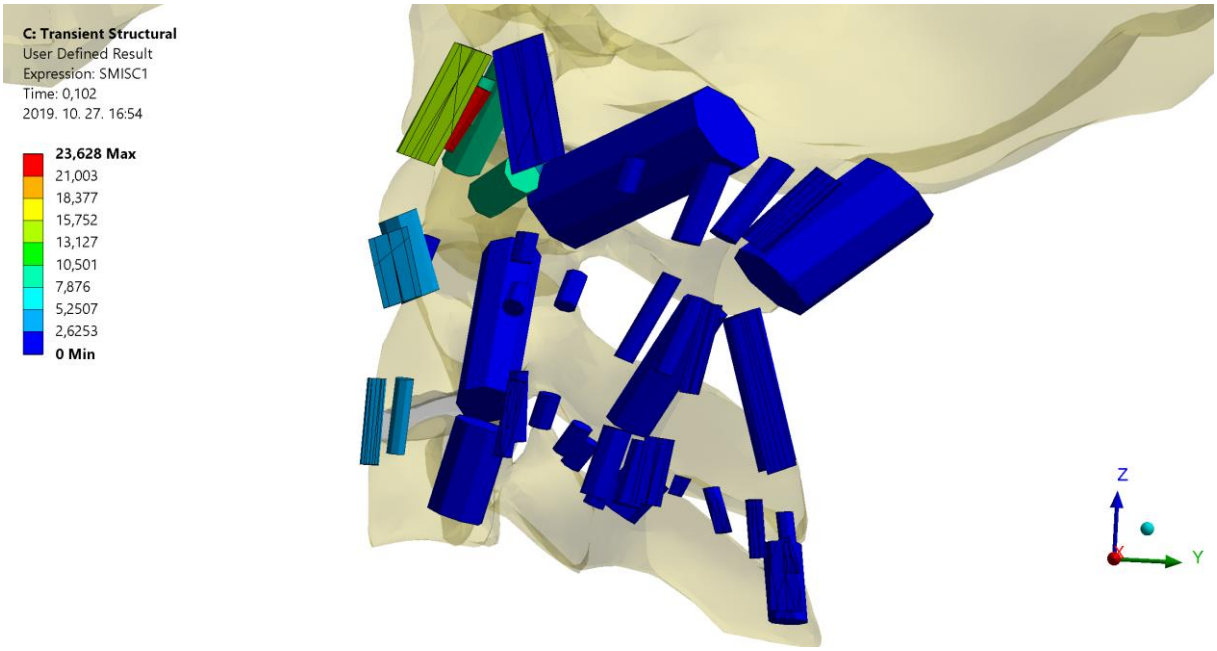

Figure 54. Cross section through the median sagittal plane: axial forces [N] of LINK180 elements of muscles and ligaments at time 0,102 s

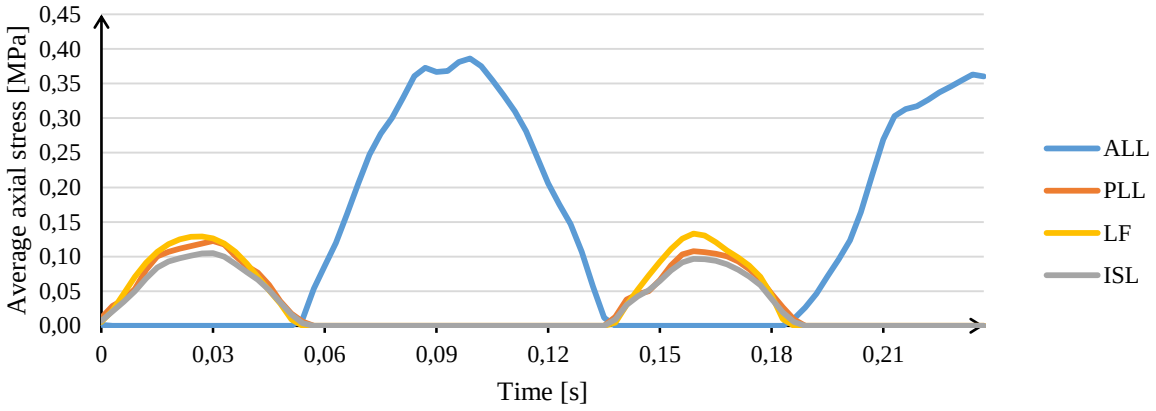

Figure 55. Average axial stress [MPa] of different ligaments

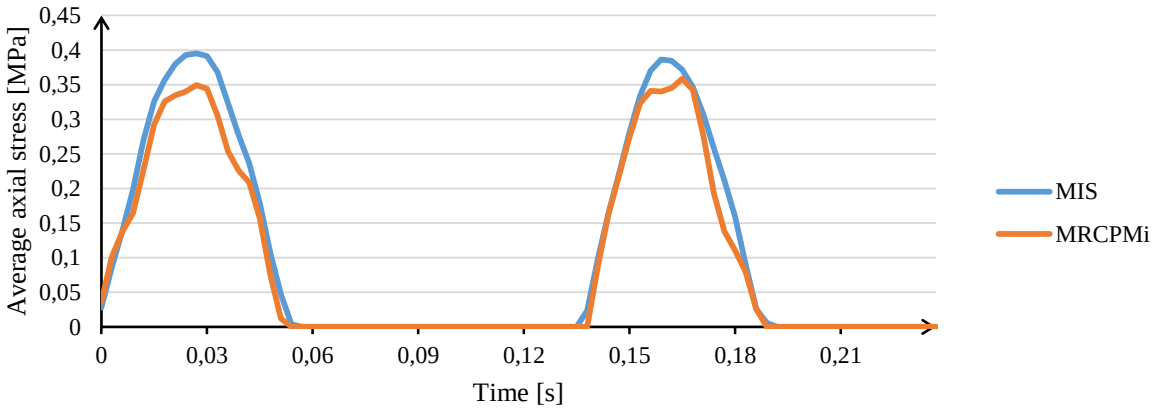

Figure 56. Average axial stress [MPa] of different muscles

6. CONCLUSIONS

As a first step of further investigations, a simplified model of the head-neck complex was developed that consists of the skull without the mandible, the top three vertebrae, the intervertebral disc between C2 and C3, most of the ligaments, and a few pair of deep muscle.

During the preliminary analyses, a few discrepancies made themselves evident. One essential issue is the contact definition between separate solid bodies. For instance, the cranium has the capability of rotating around the frontal axis, gliding on its occipital condyles. The range of this motion is large therefore it cannot be neglected. The presented model is not capable of exhibiting the same behavior due to the artificial cartilage-like solids connecting C1 and the skull. Consequently, most of the rotation was produced by the deformation of the intervertebral disc between C2 and C3. As far as the top two vertebrae are concerned, a bonded contact is apparently not sufficient of modelling the connection of these vertebrae. Additionally, the articular surfaces of adjacent vertebrae may also likely come in contact with one another therefore a frictionless contact ought to be defined.

Furthermore, the results suggest that the model response is sensitive to the distribution of the soft tissues. This does not necessarily mean that one should avoid any asymmetry during modelling. The human body – and any living being – has the inevitable property of being slightly asymmetric. The effect of lacking perfect symmetry is worth exploring. However, in this model's case, this much asymmetry in the results may be considered as an indication of modelling inaccuracy. The asymmetric position of MOCS may likely exceed the natural asymmetry thus a correction of the model is due (**Figure 38. b**)

Taking into account some of the soft tissues with the help of cable elements maybe sufficient in some cases. In reality however, ligaments and muscles are always in at least modest tension therefore a pre-stressed state of these soft tissues would presumably improve the model response. Including material nonlinearity of soft tissues would affect model response accuracy to a large extent. Also, modelling soft tissues with the help of 2D or 3D elements would enhance the model's capability of analyzing the response of the neck in much more detail.

7. REFERENCES

ANSYS Mechanical. (2018). en, Ansys, Inc., Canonsburg, Pennsylvania, USA.

ANSYS SpaceClaim. (2018). en, Ansys, Inc., Canonsburg, Pennsylvania, USA.

Bankoff, A. D. P. (2012). "Biomechanical Characteristics of the Bone." *Human Musculoskeletal Biomechanics*, T. Goswami, ed., InTech.

Barclay, T. (2019). "Muscular System - Muscles of the Human Body." *Innerbody*, <https://www.innerbody.com/image/musfov.html> (Oct. 8, 2019).

Betts, J. G., Desaix, P., Johnson, E., Johnson, J. E., Korol, O., Kruse, D., Poe, B., Wise, J. A., Womble, M., and Young, K. A. (2013). *Anatomy & Physiology*. Rice University, Texas.

Bogduk, N., and Mercer, S. (2000). "Biomechanics of the cervical spine. I: Normal kinematics." *Clinical Biomechanics*, 16.

Borst, J., Forbes, P. A., Happee, R., and Veeger, D. (H. E. J.). (2011). "Muscle parameters for musculoskeletal modelling of the human neck." *Clinical Biomechanics*, 26(4), 343–351.

Bredbenner, T. L., Eliason, T. D., Francis, W. L., McFarland, J. M., Merkle, A. C., and Nicolella, D. P. (2014). "Development and Validation of a Statistical Shape Modeling-Based Finite Element Model of the Cervical Spine Under Low-Level Multiple Direction Loading Conditions." *Frontiers in Bioengineering and Biotechnology*, 2.

Brolin, K., Halldin, P., and Leijonhufvud, I. (2005). "The Effect of Muscle Activation on Neck Response." *Traffic Injury Prevention*, 6(1), 67–76.

Brolin, K., Hedenstierna, S., Halldin, P., Bass, C., and Alem, N. (2008). "The importance of muscle tension on the outcome of impacts with a major vertical component." *International Journal of Crashworthiness*, 13(5), 487–498.

de Bruijn, E., van der Helm, F. C. T., and Happee, R. (2016). "Analysis of isometric cervical strength with a nonlinear musculoskeletal model with 48 degrees of freedom." *Multibody System Dynamics*, 36(4), 339–362.

Chancey, V. C., Nightingale, R., Van Ee, C., E Knaub, K., and S Myers, B. (2003). "Improved estimation of human neck tensile tolerance: Reducing the range of reported tolerance using anthropometrically correct muscles and optimized physiologic initial conditions." *Stapp Car Crash Journal*, 47, 135–53.

Chazal, J., Tanguy, A., Bourges, M., Gaurel, G., Escande, G., Guillot, M., and Vanneuville, G. (1985). "Biomechanical properties of spinal ligaments and a histological study of the supraspinal ligament in traction." *Journal of Biomechanics*, 18(3), 167–176.

Chen, H., Zhang, L., Wang, Z., Yang, K., and King, A. (2011). "Biomechanics of the Neck." *Theoretical Biomechanics*, V. Klika, ed., 385–402.

Choi, H. Y., Lee, I. H., Haug, E., Takhounts, E., and Eppinger, R. (2002). "Development of Finite Element Human Neck Model for the SIMON Program." *Proceedings of the Thirty-Ninth Injury Biomechanics Research International Workshop*.

Clark, J. G., Abdullah, K. G., Mroz, T. E., and Steinmetz, M. P. (2011). "Biomechanics of the Craniovertebral Junction." *Biomechanics in Applications*.

Clauser, C., McConville, J., and Young, J. W. (1969). *Weight, Volume, and Center of Mass of Segments of the Human Body*. Air Force Systems Command Wright- Patterson Air Force Base, Ohio, 112.

Cusick, J., and Yoganandan, N. (2002). "Biomechanics of the cervical spine 4: Major injuries." *Clinical Biomechanics*, 17(1), 1–20.

DeWit, J. A., and Cronin, D. S. (2010). "Cervical Spine Segment Finite Element Model Validation and Verification at Traumatic Loading Levels for Injury Prediction." 12.

Dibb, A., Nightingale, R., Luck, J., Carol Chancey, V., E Fronheiser, L., and S Myers, B. (2009). "Tension and Combined Tension-Extension Structural Response and Tolerance Properties of the Human Male Ligamentous Cervical Spine." *Journal of biomechanical engineering*, 131, 081008.

Dibb, A. T., Cox, C. A., Nightingale, R. W., Luck, J. F., Cutcliffe, H. C., Myers, B. S., Arbogast, K. B., Seacrist, T., and Bass, C. R. (2013). "Importance of Muscle Activations for Biofidelic Pediatric Neck Response in Computational Models." *Traffic Injury Prevention*, 14(sup1), S116–S127.

Dibb, A. T., Narvekar, A., Nightingale, R. W., and Myers, B. S. (2007). "A Comparison of Methods for Modeling Neck Muscle Wrapping in Finite Element Models." *Proceedings of the Thirty-Fifth Injury Biomechanics Research International Workshop*.

Fice, J. B., Moulton, J. A., and Cronin, D. S. (2011). "Development of a Detailed Finite Element Neck Model for Automotive Safety Research." *Proceedings of the Thirty-Ninth Injury Biomechanics Research International Workshop*.

French, D. D., Campbell, R. R., Sabharwal, S., Nelson, A. L., Palacios, P. A., and Gavin-Dreschnack, D. (2007). "Health Care Costs for Patients With Chronic Spinal Cord Injury in the Veterans Health Administration." *The Journal of Spinal Cord Medicine*, 30(5), 477–481.

Freutel, M., Schmidt, H., Dürselen, L., Ignatius, A., and Galbusera, F. (2014). "Finite element modeling of soft tissues: Material models, tissue interaction and challenges." *Clinical Biomechanics*, 29(4), 363–372.

Goel, V. K., Clark, C. R., Gallaes, K., and Liu, Y. K. (1988). "Moment-rotation relationships of the ligamentous occipito-atlanto-axial complex." *Journal of Biomechanics*, 21(8), 673–680.

Goel, V. K., Clark, C. R., McGowan, D., and Goyal, S. (1984). "An in-vitro study of the kinematics of the normal, injured and stabilized cervical spine." *Journal of Biomechanics*, 17(5), 363–376.

Golinski, W. Z., and Gentle, C. R. (2001). "Biomechanical simulation of whiplash - some implications for seat design." *International Journal of Crashworthiness*, 6(4), 573–584.

Gray, H. (1918). *Anatomy of the Human Body*. Lea & Febiger, Philadelphia.

Greaves, C. Y., Gadala, M. S., and Oxland, T. R. (2008). "A Three-Dimensional Finite Element Model of the Cervical Spine with Spinal Cord: An Investigation of Three Injury Mechanisms." *Annals of Biomedical Engineering*, 36(3), 396.

Hamer, S. (2018). "Human Anatomy V3 - Male (Life Sciences Japan, BodyParts3D Source)." *GrabCAD*, <https://grabcad.com/library/human-anatomy-v3-male-life-sciences-japan-bodyparts3d-source-1> (Aug. 5, 2019).

Han, I. S., Kim, Y. E., and Jung, S. (2012). "Finite element modeling of the human cervical spinal column: Role of the uncovertebral joint." *Journal of Mechanical Science and Technology*, 26(6), 1857–1864.

Hedenstierna, S. (2008). "3D Finite Element Modeling of Cervical Musculature and its Effect on Neck Injury Prevention." Royal Institute of Technology, Stockholm.

Herbert, R. (1988). "The Passive Mechanical Properties of Muscle and Their Adaptations to Altered Patterns of Use." *Australian Journal of Physiotherapy*, 34(3), 141–149.

Hill, A. V. (1938). "The heat of shortening and the dynamic constants of muscle." *Proceedings of the Royal Society of London. Series B - Biological Sciences*, 126(843), 136–195.

Hines, T. (2018). "Anatomy of the Spine."

van der Horst, M. J., Thunnissen, J., Happee, R., Haaster, R., and Wismans, J. (1997). "Influence of muscle activity on head-neck response during impact." *Stapp Car Crash Conference Proceedings*.

Ivancic, P. C., Coe, M. P., Ndu, A. B., Tominaga, Y., Carlson, E. J., Rubin, W., (FH), D.-I., and Panjabi, M. M. (2007). "Dynamic Mechanical Properties of Intact Human Cervical Spine Ligaments." *The spine journal : official journal of the North American Spine Society*, 7(6), 659–665.

Jefferson, G. (1919). "Fracture of the atlas vertebra. Report of four cases, and a review of those previously recorded." *BJS*, 7(27), 407–422.

Jones, O. (2012). "Anatomical Planes." *TeachMeAnatomy*, <https://teachmeanatomy.info/the-basics/anatomical-terminology/planes/> (Apr. 22, 2019).

Jost, R., and Nurick, G. N. (2000). "Development of a finite element model of the human neck subjected to high g-level lateral deceleration." *International Journal of Crashworthiness*, 5(3), 259–270.

Jovanović, K., Vranić, J., and Miljković, N. (2015). "Hill's and Huxley's muscle models - tools for simulations in biomechanics." *Serbian Journal of Electrical Engineering*, 12(1), 53–67.

Kandziora, F., Schnake, K., and Hoffmann, R. (2010). "Injuries to the upper cervical spine. Part 2: Osseous injuries." *Der Unfallchirurg*, 113(12), 1023–1041.

King, A. I. (2018a). "Impact Biomechanics of Neck Injury." *The Biomechanics of Impact Injury: Biomechanical Response, Mechanisms of Injury, Human Tolerance and Simulation*, A. I. King, ed., Springer International Publishing, Cham, 201–241.

King, A. I. (2018b). "Biomechanics of Sports Injuries." *The Biomechanics of Impact Injury: Biomechanical Response, Mechanisms of Injury, Human Tolerance and Simulation*, A. I. King, ed., Springer International Publishing, Cham, 629–647.

Klein Breteler, M. D., Spoor, C. W., and Van der Helm, F. C. T. (1999). "Measuring muscle and joint geometry parameters of a shoulder for modeling purposes." *Journal of Biomechanics*, 32(11), 1191–1197.

Korhonen, R. K., and Saarakkala, S. (2011). "Biomechanics and Modeling of Skeletal Soft Tissues." *Theoretical Biomechanics*, V. Klika, ed.

Kumar, S., Ferrari, R., and Narayan, Y. (2005). "Analysis of right anterolateral impacts: the effect of head rotation on the cervical muscle whiplash response." *Journal of NeuroEngineering and Rehabilitation*, 2, 11.

Kumar, S., Ferrari, R., Narayan, Y., and Vieira, E. (2006). "Analysis of right anterolateral impacts: the effect of trunk flexion on the cervical muscle whiplash response." *Journal of NeuroEngineering and Rehabilitation*, 3, 10.

Kumaresan, S., Yoganandan, N., Pintar, F. A., and Mueller, W. M. (2000). "Biomechanics of Pediatric Cervical Spine: Compression, Flexion and Extension Responses." *Journal of Crash Prevention and Injury Control*, 2(2), 87–101.

Kurutz, M. (2010). "Finite Element Modelling of Human Lumbar Spine." *Finite Element Analysis*, D. Moratal, ed., Sciyo, 209–236.

Landínez-Parra, N. S., Garzón-Alvarado, D. A., and Vanegas-Acosta, J. C. (2012). "Mechanical Behavior of Articular Cartilage." *Injury and Skeletal Biomechanics*.

Lowe, R., Ritchie, L., Thomas, E., van der Stockt, T., and Buxton, S. (2018). "Cardinal Planes and Axes of Movement." *Physiopedia*, <https://www.physio-pedia.com/Cardinal_Planes_and_Axes_of_Movement> (May 31, 2019).

Lucas, S. R., Bass, C. R., Salzar, R. S., Oyen, M. L., Planchak, C., Ziemba, A., Shender, B. S., and Paskoff, G. (2008). "Viscoelastic properties of the cervical spinal ligaments under fast strain-rate deformations." *Acta Biomaterialia*, 4(1), 117–125.

Mattucci, S. F. E., and Cronin, D. S. (2015). "A method to characterize average cervical spine ligament response based on raw data sets for implementation into injury biomechanics models." *Journal of the Mechanical Behavior of Biomedical Materials*, 41, 251–260.

Mattucci, S. F. E., Moulton, J. A., Chandrashekar, N., and Cronin, D. S. (2012). "Strain rate dependent properties of younger human cervical spine ligaments." *Journal of the Mechanical Behavior of Biomedical Materials*, 10, 216–226.

Mattucci, S. F. E., Moulton, J. A., Chandrashekar, N., and Cronin, D. S. (2013). "Strain rate dependent properties of human craniovertebral ligaments." *Journal of the Mechanical Behavior of Biomedical Materials*, 23, 71–79.

Meyer, F., Bourdet, N., Deck, C., Willinger, R., and Raul, J. S. (2004). "Human Neck Finite Element Model Development and Validation against Original Experimental Data."

Meyer, F., Bourdet, N., Gunzel, K., and Willinger, R. (2013). "Development and validation of a coupled head-neck FEM – application to whiplash injury criteria investigation." *International Journal of Crashworthiness*, 18(1), 40–63.

Mitsuhashi, N., Fujieda, K., Tamura, T., Kawamoto, S., Takagi, T., and Okubo, K. (2009). "BodyParts3D: 3D structure database for anatomical concepts." *Nucleic Acids Research*, 37(Database issue), D782–D785.

Natali, A. N., and Meroi, E. A. (1989). "A review of the biomechanical properties of bone as a material." *Journal of Biomedical Engineering*, 11(4), 266–276.

Newell, N., Little, J., Christou, A., Adams, M., Adam, C., and Masouros, S. (2017). "Biomechanics of the human intervertebral disc: A review of testing techniques and results." *Journal of the Mechanical Behavior of Biomedical Materials*, 69, 420–434.

Nightingale, R. W., Myers, B. S., and Yoganandan, N. (2015). "Neck Injury Biomechanics." *Accidental Injury*, The Medical College of Wisconsin Inc on behalf of Narayan Yoganandan, N. Yoganandan, A. M. Nahum, and J. W. Melvin, eds., Springer New York, New York, NY, 259–308.

Oftadeh, R., Perez-Viloria, M., Villa-Camacho, J. C., Vaziri, A., and Nazarian, A. (2015). "Biomechanics and Mechanobiology of Trabecular Bone: A Review." *Journal of Biomechanical Engineering*, 137(1), 0108021–01080215.

Östh, J., Brolin, K., Svensson, M. Y., and Linder, A. (2016). "A Female Ligamentous Cervical Spine Finite Element Model Validated for Physiological Loads." *Journal of Biomechanical Engineering*, 138(6), 061005-061005–9.

Pal, S. (2014). "Mechanical Properties of Biological Materials." *Design of Artificial Human Joints & Organs*, Springer, New York.

Pan, C.-Y., Liu, P.-H., Tseng, Y.-C., Chou, S.-T., Wu, C.-Y., and Chang, H.-P. (2019). "Effects of cortical bone thickness and trabecular bone density on primary stability of orthodontic mini-implants." *Journal of Dental Sciences*.

Pandy, M. G., and Barr, R. E. (2004). "Biomechanics of the Musculoskeletal System." *Standard Handbook of Biomedical Engineering and Design*, McGraw-Hill standard handbooks, M. Kutz, R. Adrezin, R. Barr, C. Batich, R. Bellamkonda, A. Brammer, T. Buchanan, A. Cook, J. Curie, and A. Dolan, eds., McGraw-Hill, New York, 34.

Panzer, M. B. (2006). "Numerical Modelling of the Human Cervical Spine in Frontal Impact." University of Waterloo, Waterloo.

Panzer, M. B., Fice, J. B., and Cronin, D. S. (2011). "Cervical spine response in frontal crash." *Medical Engineering & Physics*, 33(9), 1147–1159.

Pintar, F. A., Voo, L. M., Yoganandan, N., Cho, T. H., and Maiman, D. J. (1998). "Mechanisms of Hyperflexion Cervical Spine Injury." 12.

Pugh, J. W., Rose, R. M., and Radin, E. L. (1973). "Elastic and viscoelastic properties of trabecular bone: Dependence on structure." *Journal of Biomechanics*, 6(5), 475–485.

Sokol, M., Velísková, P., Rehák, Ľ., and Žabka, M. (2014). "Three-Dimensional Mechanical Model of the Human Spine and the Versatility of its Use." *Slovak Journal of Civil Engineering*, 22(1), 37–42.

"Structure of Skeletal Muscle." (n.d.). *SEER Training Modules*, <https://www.training.seer.cancer.gov/anatomy/muscular/structure.html> (Oct. 9, 2019).

Subramani, V., and Justin, J. (2016). "The Development and Analysis of a Finite Element Model of the C45 Cervical Spine Segment." 22.

Szentágothai J., and Réthelyi M. (2006). *Funkcionális anatómia I.* Budapest.

Teixeira, T., Sousa, L. C., Natal Jorge, R. M., Parente, M., Gonçalves, J. M., and Freitas, R. (2015). "Biomechanical Study of the Cervical Spine." *Computational and Experimental Biomedical Sciences: Methods and Applications*, J. M. R. S. Tavares and R. M. Natal Jorge, eds., Springer International Publishing, Cham, 91–103.

Teo, E. C., Zhang, Q. H., and Huang, R. C. (2007). "Finite element analysis of head–neck kinematics during motor vehicle accidents: Analysis in multiple planes." *Medical Engineering & Physics*, 29(1), 54–60.

Toosizadeh, N., and Haghpanahi, M. (2011). "Generating a finite element model of the cervical spine: Estimating muscle forces and internal loads." *Scientia Iranica*, 18(6), 1237–1245.

Trajkovski, A., Omerović, S., Hribernik, M., and Prebil, I. (2014a). "Failure Properties and Damage of Cervical Spine Ligaments, Experiments and Modeling." *Journal of Biomechanical Engineering*, 136(3), 031002-031002–9.

Trajkovski, A., Omerovic, S., Krasna, S., and Prebil, I. (2014b). "Loading rate effect on mechanical properties of cervical spine ligaments." 8.

Troyer, K. L., and Puttlitz, C. M. (2011). "Human cervical spine ligaments exhibit fully nonlinear viscoelastic behavior." *Acta Biomaterialia*, 7(2), 700–709.

Troyer, K. L., and Puttlitz, C. M. (2012). "Nonlinear viscoelasticity plays an essential role in the functional behavior of spinal ligaments." *Journal of Biomechanics*, 45(4), 684–691.

Wagner, D. R., and Lotz, J. C. (2004). "Theoretical model and experimental results for the nonlinear elastic behavior of human annulus fibrosus." *Journal of Orthopaedic Research*, 22(4), 901–909.

Wang, Y. W., Wang, L. Z., Liu, S. Y., and Fan, Y. B. (2018). "A two-step procedure for coupling development and usage of a pair of human neck models." *Computer Methods in Biomechanics and Biomedical Engineering*, 21(5), 413–426.

Wei, W., Liu, Y., Du, X., and Li, N. (2017). "Development and validation of a C0-C7 cervical spine finite element model." *MATEC Web of Conferences*, 108, 13007.

Weiss, J. A., Gardiner, J. C., and Bonifasi-Lista, C. (2002). "Ligament material behavior is nonlinear, viscoelastic and rate-independent under shear loading." *Journal of Biomechanics*, 35(7), 943–950.

Wheeldon, J. A., Pintar, F. A., Knowles, S., and Yoganandan, N. (2006). "Experimental flexion/extension data corridors for validation of finite element models of the young, normal cervical spine." *Journal of Biomechanics*, 39(2), 375–380.

Wheeldon, J. A., Stemper, B. D., Yoganandan, N., and Pintar, F. A. (2008). "Validation of a Finite Element Model of the Young Normal Lower Cervical Spine." *Annals of Biomedical Engineering*, 36(9), 1458–1469.

Yoganandan, N., Kumaresan, S., and Pintar, F. A. (2000). "Geometric and Mechanical Properties of Human Cervical Spine Ligaments." *Journal of Biomechanical Engineering*, 122(6), 623.

Yoganandan, N., Kumaresan, S., and Pintar, F. A. (2001). “Biomechanics of the cervical spine Part 2. Cervical spine soft tissue responses and biomechanical modeling.” *Clinical Biomechanics*, 16(1), 1–27.

Zafarparandeh, I., Erbulut, D. U., and Ozer, A. F. (2016). “Influence of three-dimensional reconstruction method for building a model of the cervical spine on its biomechanical responses: A finite element analysis study.” *Advances in Mechanical Engineering*, 8(3), 168781401663880.

Zhang, J.-G., Wang, F., Zhou, R., and Xue, Q. (2011). “A three-dimensional finite element model of the cervical spine: an investigation of whiplash injury.” *Medical & Biological Engineering & Computing*, 49(2), 193–201.

Zhang, Q. H., Teo, E. C., and Ng, H. W. (2005). “Development and Validation of A C0–C7 FE Complex for Biomechanical Study.” *Journal of Biomechanical Engineering*, 127(5), 729–735.